CHAPTER 3

CLASSICAL COUPLED PLASTICITY AND DAMAGE THEORY

3.1 Introduction

The nonlinear material behavior may be attributed to two distinct material mechanical processes: plasticity (i.e. dislocations along crystal slip planes) and damage mechanics (microcracks, microcavities nucleation and coalescence, decohesions, grain boundary cracks, and cleavage in regions of high stress concentration). The two degradation phenomena are described best by the continuum theories of plasticity and damage mechanics. Thus, a multi-dissipative model that accounts for both the material decohesions and the dislocations along slip planes is necessary. This is accomplished by adopting two loading surfaces and two potential functions, one for plasticity and the other for damage.

Ductile materials usually fail as the result of nucleation, growth, and coalescence of microdamages. Experimental observations show that the accumulation of microdamages has a tendency to form macroscopically localized damage, which is a precursor to failure. This progressive physical process of degradation of the material mechanical properties up to complete failure is commonly referred to as damage. Various damage morphologies have been described in the literature, such as creep damage, low cycle fatigue, high cycle fatigue, and brittle damage (Kachanov, 1986; Lemaitre and Chaboche, 1990; Lemaitre, 1992; Voyiadjis and Kattan, 1999). The present paper is concerned with anisotropic ductile damage.

Metallographic studies for polycrystalline metals (Thomason, 1990; Anderson, 1994; Hertzberg, 1996) demonstrate that the ductile damage is basically characterized by three mechanisms of microdamages growth: (i) nucleation of microscopic voids that initiate at inclusions and second phase particles, failure of particles or microcracking of the matrix surrounding the inclusion, (ii) growth of the microvoids by means of plastic strain and hydrostatic stress; and (iii) coalescence or microcracks linking the growing microvoids with adjacent ones, thus leading to vanishing load carrying capacity of the material, as the damage density approaches unity.

Many models for estimating the microdamage accumulation in ductile materials have been published, some of which are based on damage micromechanics (*micromechanical damage models*) while others based on the continuum damage theory (*phenomenological damage models*). The former models are required for particles of less than $1\,\mu m$ in diameter. A model of this type was formulated by Gurson (1977), where he obtained, based on an approximation analysis of spherical voids, a yield function for porous ductile materials with perfectly plastic matrix. Modification of the Gurson's model have been proposed by several authors (e.g. Tvergaard, 1982; Tvergaard and Needleman, 1984). Tvergaard (1982) modified Gurson's model to improve the predictions at low void volume fractions. Tvergaard and Needleman (1984) modified Gurson's yield function in order to account for rate sensitivity and necking instabilities in plastically deforming solids and to provide better representation of final void coalescence. The aspects of Gurson's model was outlined in the review article by Nemat-Nasser (1992) and discussed by Voyiadjis and Kattan (1992a,b), Li (2000), and Mahnken (2002). In this way micromechanical models are based on physical soundness, and various

structural applications have modeled microdamage growth and ductile failure (Haj-Ali et al., 2001).

Phenomenological models are based on the concept of Kachanov (1958), who was the first to introduce for the isotropic case a one-dimensional variable, which may be interpreted as the effective surface density of microdamages per unit volume (Voyiadjis and Venson, 1995; Venson and Voyiadjis, 2001). Kachanov (1958) pioneered the subject of continuum damage mechanics by introducing the concept of effective stress. This concept is based on considering a fictitious undamaged configuration of a body and comparing it with the actual damaged configuration. He originally formulated his theory on simple uniaxial tension bars. Following Kachanov's work researchers in different fields applied continuum damage mechanics to brittle materials (Krajcinovic and Foneska, 1981; Krajcinovic, 1983, 1996) and ductile materials (Lemaitre, 1984, 1985; Kachanov, 1986; Murakami, 1988). In the 1990's numerous applications of continuum damage mechanics to plasticity were presented (e.g. Lubarda and Krajcinovic, 1995; Voyiadjis and Kattan, 1992a, 1992b, 1999; Voyiadjis and Park, 1997, 1999; Voyiadjis and Deliktas, 2000; etc).

Often, ductile materials undergo a strong plastic deformation, which has a major influence on the damage evolution and reverse. There are many models with weak coupling between plasticity and damage. The models that adopt two separate uncoupled damage and plastic loading surfaces with two independent associated flow rules present a week coupling between plasticity and damage. Those models are being extensively used by many authors (e.g. Chow and Wang, 1987, 1988; Simo and Ju, 1989; Lemaitre and Chaboche, 1990; Hansen and Schreyer, 1994; Zhu and Cescetto, 1995; Murakami et al., 1998; etc.). While there are many models with weak coupling, no consistent model realizing a strong coupling has been published yet. However, relatively strong coupling between plasticity and damage can be achieved by using one single smooth generalized yield surface and an associated flow rule for the plasticity and damage evolutions (e.g. Gurson, 1977; Tvergaard, 1982; Tvergaard and Needleman, 1984; Rousselier, 1987; Ehlers, 1995; Hesebeck, 2001; Mahnken, R., 2002). Those models obviously cannot describe all loadings correctly since a hydrostatic stress will certainly cause damage before any plastic deformation can be noticed. In addition most of those models are restricted to low damage levels or dilute distribution of defects and therefore they fail to account for the interaction of the defects adequately. Another approach to achieve this strong coupling is by using separate plasticity and damage surfaces with separate non-associated flow rules in such a way that both damage and plasticity flow rules are dependent on both the plastic and damage potentials (Voyiadjis and Deliktas, 2000). The later approach is adopted in this work, where the strong coupling between plasticity and damage is implemented by using two damage mechanisms. One mechanism is coupled with plasticity, while the other occurs independent of the plastic deformation. The dissipation function of the latter occurs in both the elastic and plastic domains. To formulate that on the basis of the thermodynamic principles, the two damage processes are represented using two additive components in the dissipation potential. Since this work focuses on the development of coupled plastic-damage governing equations based on thermomechanical postulates, the various possibilities to describe plasticity and anisotropic damage behavior in materials shall be considered here.

It is generally assumed that the rate of deformation can be additively decomposed into an elastic (reversible) part and an inelastic (irreversible) part (e.g. Nemat-Nasser, 1983; Lubliner, 1990; Simo and Hughes, 1998). 'Non-instantaneously reversible' deformation is a more

general description of the inelastic deformation since it is corresponding to the following set of physical phenomena: instantaneous plasticity, viscoplasticity, damage, and viscodamage. The first type of inelastic deformation is a time-independent mechanism, which is generally considered in the rate-independent plasticity theories. The viscoplastic deformation, which is sometimes qualified as creep, is a rate-dependent mechanism. Both of those two mechanisms or one of them is generally not sufficient to describe the set of experimental observations. Therefore, degradation of the mechanical properties up to complete failure should be considered in the experimental simulations. The damage growth can be time-independent (damage theory) and/or time-dependent process (viscodamage theory). The evolution, nucleation, and coalescence of microcracks, voids, and cavities during manufacturing processes and subsequent loading enhance the material to behave inelastically in the elastic and plastic domains. Voyiadjis and Park (1999) summed such defects as an inelastic strain called the damage strain. They decomposed this damage strain into elastic-damage (recoverable) component attributed to crack closure and void contraction during unloading, and inelastic-damage (unrecoverable) component attributed to random distribution and orientation of the cracks that make their recovery impossible. In accordance with their work, two irreversible strains are considered in this study: the plastic and the damage strains.

An outline for the work in this chapter is as follows: In Section 3.2 we demonstrate the motivated morphologies for the additive decomposition of the total strain into elastic, plastic, and damage components. Section 3.3 is devoted to the physical interpretations of the damage variable for both the isotropic and anisotropic damage distributions. Furthermore the derivation of the energy release rate is outlined for both isotropic and anisotropic damage distributions. In Section 3.4, we outline a general thermodynamic framework for the coupled elasto-plastic and damage material behavior. In Section 3.5, the derived evolution equations are examined for pure isotropic damage case and applied to simulate computationally the experimental results of Hesebeck (2001) for high strength steel specimens subjected to tensile loading. This chapter is restricted to small strains.

3.2 The Strain Additive Decomposition

Experimental observations show that in general the processes of cold-working, forming, machining of mechanical parts, etc. can cause an initial evolution of defects in the virgin material state, such as nucleation of certain amount of cracks, voids, and dislocation patterns. The initial defects induced in the material microstructure along with the subsequent defects that occur during deformation process enhance the material to behave inelastically even before the onset of plasticity. If the material is elastically unloaded before forming dislocations along slip planes (plasticity), permanent strains are observed. Those strains are irreversible damage strains, while the reversible strains are of two parts: elastic part and damage part. As plastic deformations initiate, both damage and plastic permanent deformations are anticipated. Next we demonstrate this behavior in uniaxial tension and complex loadings.

Imagine an elastically loaded representative volume element (RVE) containing uniformly distributed (micro)-cracks of Mode I, which are triggered by the process of cold working, and is deformed by a total strain ε_1. A certain part of this strain is elastically recoverable (ε_1^e) and another part is induced by damage (ε_1^{ed}). After the loads are released before the yield limit is

reached, the body will have no permanent strains left. However, the magnitude of the elastic stiffness for the RVE maybe reduced due to the growth of microcracks. This is clearly demonstrated in Figure 3.1 which shows the foregoing micromechanics of a continuum point in the RVE and the corresponding macro-stresses and strains. We begin with an unstressed unit cell in the RVE containing a microcrack of length $2a$ and a resulting average stiffness $\bar{E}_1$ (the stiffness of the matrix surrounding the microcrack remains unchanged by microcrack opening). Up to a certain stress level, the microcrack will not grow but only open. Therefore, the microcrack length will remain $2a$ (neglecting the Poisson's effect) and the RVE average stiffness will not change. Beyond this threshold, however, the microcrack extends by an amount $2(da)$ and the average stiffness decreases by an amount dE_1. Upon the load release the microcrack will close and no further growth occurs. For the same stress (points *b* and *d*) a greater strain will result, due to the reduction in the RVE average stiffness. In the stress free state there are no permanent strains left, only the resulted average stiffness (E_1) is less than that of the initial body. The amount of the stored elastic strain energy at the end of the loading process is given by $\sigma_{1c}\left(\varepsilon_{1c}^{e}+\varepsilon_{1c}^{ed}\right)/2$ and the additional surface energy resulting from the microcrack extension by an amount of $2da$ is obtained from the work done by the applied stress $\sigma_{1c}[(\varepsilon_{1c}^{e}+\varepsilon_{1c}^{ed})-(\varepsilon_{1a}^{e}+\varepsilon_{1a}^{e})]$.

Imagine now the elastically loaded RVE containing an arbitrary distribution of (micro)-voids and (micro)-cracks of mixed modes (Mode I, II, and III), which are triggered by the process of cold working, and subjected to a 2-D state of stress. Generally, this situation is more likely to happen in materials than the former case. The RVE is deformed by a total strain of $\boldsymbol{\varepsilon}$; a certain part of it is elastically recoverable ($\boldsymbol{\varepsilon}^e$) and another part is induced by the damage ($\boldsymbol{\varepsilon}^d$). If the loads are released before yielding is observed, the body will have, similar to plasticity and in contrast to the previous fictitious situation, permanent deformations ($\boldsymbol{\varepsilon}^{id}$). Those irreversible damage strains are attributed to the necessary geometric constraints

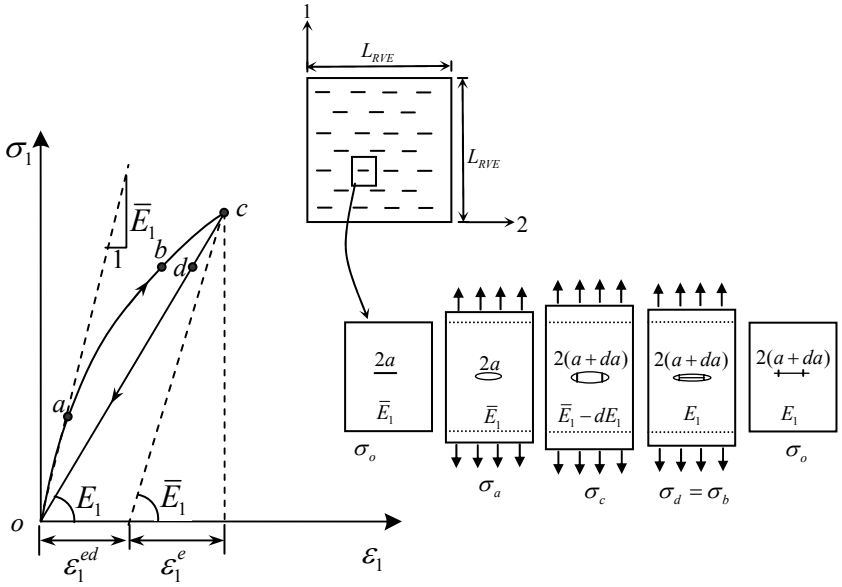

Figure 3.1. Fictitious uniaxial stress-strain elastic response resulting from a growing micro-crack. All the damage strain is recoverable (the crack is closed but not healed).

set by other (micro)-defects. Figure 3.2 shows the underlying micromechanics of a continuum point in the RVE and the corresponding macro-stresses and strains in one of the geometric directions. The existing stress state is that of combined biaxial tension and shear ($\sigma_2 > \sigma_1 > \tau_{12}$) with the stress-strain behavior in the 2-directions being accounted for. We start with an unstressed sub-RVE containing a growing microcrack and microvoid with an average stiffness $\bar{\boldsymbol{E}}$ (the stiffness of the matrix surrounding the microcrack/microvoid remains unchanged by the microcrack opening). Up to a certain stress level, the microcrack will open and start growing and the microvoid will expand. This process is accompanied by shape change and reduction in the average stiffness, $d\boldsymbol{E}$. Upon the loads release, part of the microcrack will close, the size of the microvoid will decrease, and no further growth occurs. For the same stress (points *b* and *d*) a greater strain will result, due to the microcrack and microvoid growth and the reduction in the average stiffness. In the stress free state, permanent strains occur and the resulted average stiffness ($\boldsymbol{E}$) is less than that of the initial body. Part of the resulted damage strain, $\boldsymbol{\varepsilon}^d$, is recovered and another part is permanent. As clearly seen, the recoverable part, $\boldsymbol{\varepsilon}^{ed}$, is attributed to partial closure of microcracks and size reduction of microvoids upon unloading (but not healing), while the unrecoverable part is attributed to lack of closure of all microcracks and unvanishing microvoids that cause permanent deformation. As we stated earlier, this may be due to the geometrical constraints set up by the interacting microcracks, microvoids, and grain boundaries.

Both situations are likely to happen under different types of loading. However, the first situation is more likely to happen in uniaxial tension, while the second situation is likely to happen in complex loading.

One now investigates the total basic one-dimensional behavior in a ductile material. Consider the uniaxial tension test shown in Figure 3.3. In this test, a bar of uniform cross-

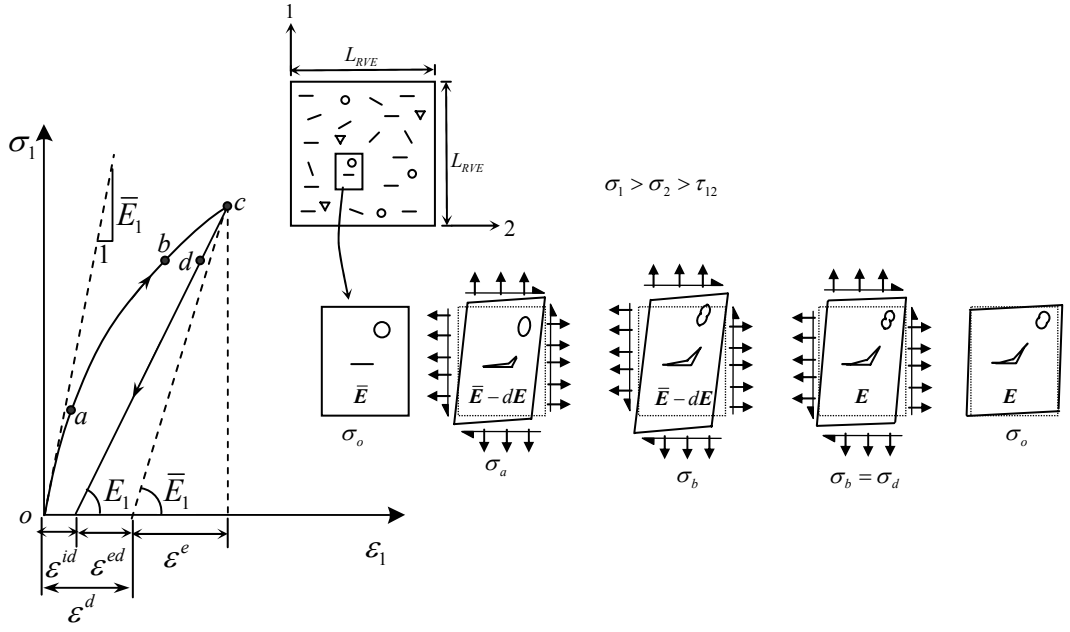

Figure 3.2 Fictitious stress-strain elastic response of an RVE subjected to a 2-D state of stress ($\sigma_1 > \sigma_2 > \tau_{12}$) resulting from a growing microcrack and microvoid. Part of the damage strain is recoverable (not healed) and the other part is unrecoverable.

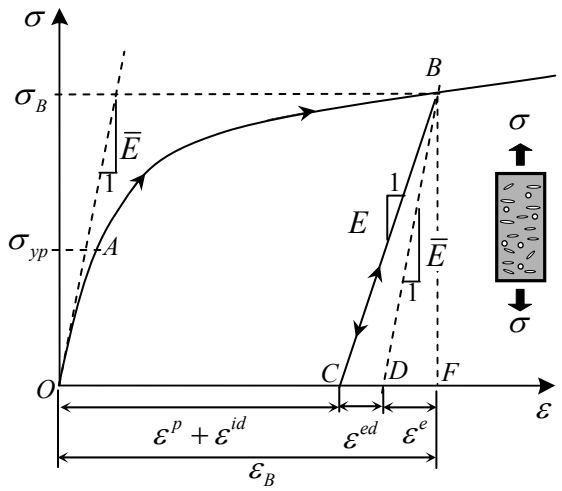

Figure 3.3 Uniaxial stress-strain response of a metallic specimen.

section is subjected to the uniaxial loading-unloading history: $O \to B \to C$, during which the length of the bar takes the following values: $L \to l^p \to l^{pid} \to l^{pd} \to l$. Stage $O \to B$ corresponds to a monotonic loading beyond the elasticity domain, and $B \to C$ to elastic unloading ($C \to B$ corresponds to elastic loading process). State C corresponds to a stress-free, unloaded configuration. We can write the following identity:

$$\frac{l}{L} = \frac{l}{l^{pd}} \frac{l^{pd}}{l^p} \frac{l^p}{L} \tag{3.1}$$

or

$$\lambda = \lambda^e \lambda^d \lambda^p \tag{3.2}$$

where $\lambda = l/L$ is the axial stretch ratio at the end of $O \to B$, $\lambda^e = l/l^{pd}$ can be viewed as the elastic stretch at the end of the elastic transformation $B \to F$, $\lambda^d = l^{pd}/l^p$ corresponds to the damage stretch between D state and a damage-free state between C and O, and $\lambda^p = l^p/L$ corresponds to plastic stretch between O state and a plastic-free state between C and O. The term "*between C and O*" is used due to the fact that part of the permanent deformation is contributed by plasticity and part from the non-recoverable damage.

Note that the superscripts here do not imply tensorial indices but merely indicate the corresponding deformation configuration such as "*e*" for elastic, "*p*" for plastic, "*d*" for damage, "*ed*" for elastic-damage, "*id*" for inelastic-damage, and "*pid*" for plastic-inelastic-damage

Additionally λ^d can be written as:

$$\frac{l^{pd}}{l^p} = \frac{l^{pd}}{l^{pid}} \frac{l^{pid}}{l^p} \tag{3.3}$$

or

$$\lambda^{d} = \lambda^{ed}\lambda^{id} \tag{3.4}$$

where $\lambda^{ed} = l^{pd}/l^{pid}$ is the elastic-damage stretch (recoverable damage stretch) between states $D \to C$, and $\lambda^{id} = l^{pid}/l^{p}$ is the unrecoverable damage stretch between C state and a damage-free state between C and O. No effective configurations are used to interpret the above definitions.

In the context of the kinematic linear theory of deformation (infinitesimal deformation) and motivated by the above schematic illustration, by the micromechanics of single crystal plasticity (Nemat-Nasser, 1979 and 1983), and the continuum damage mechanics (Voyiadjis and Park, 1999), one can assume the additive decomposition of the total strain (ε) into elastic (ε^{e}), plastic (ε^{p}), and damage components (ε^{d}). Although the damage process is an irreversible deformation thermodynamically; however, the deformation due to damage itself can be partially or completely recovered upon unloading. Thus, the damage strain component is also decomposed into elastic (reversible) and inelastic (irreversible) parts. The recoverable part is attributed to cracks closure upon unloading (but not healing), while the unrecoverable part is attributed to unclosed cracks and voids that cause permanent deformation. This may be due to the constraints set up by the interacting (micro)-cracks, (micro)-voids, dislocation densities, and grain boundaries. Both reversible and irreversible parts cause degradation in the material stiffness. Hence, in small strain theory, the total strain can be additively decomposed as:

$$\varepsilon_{ij} = \varepsilon_{ij}^{e} + \varepsilon_{ij}^{p} + \varepsilon_{ij}^{d} \tag{3.5}$$

and

$$\varepsilon_{ij}^{d} = \varepsilon_{ij}^{ed} + \varepsilon_{ij}^{id} \tag{3.6}$$

where $\boldsymbol{\varepsilon}^{ed}$ and $\boldsymbol{\varepsilon}^{id}$ are the elastic-damage and inelastic-damage parts of the damage strain, respectively. In this work the subscripted letters after the variables indicate the tensorial nature of the variables unless specifically stated otherwise.

During the unloading process, two types of strains are purely reversible: the ordinary elastic strain, ε^{e}, and the elastic-damage strain, ε^{ed}. Thus, the total reversible elastic strain, ε^{E}, due to unloading can be obtained by:

$$\varepsilon_{ij}^{E} = \varepsilon_{ij}^{e} + \varepsilon_{ij}^{ed} \tag{3.7}$$

On the other hand, the total inelastic strain, $\boldsymbol{\varepsilon}^{I}$, arises from the two irreversible sources: inelastic damage and plastic flow such that:

$$\varepsilon_{ij}^{I} = \varepsilon_{ij}^{id} + \varepsilon_{ij}^{p} \tag{3.8}$$

Eq. (3.5) can therefore be expressed as follows:

$$\varepsilon_{ij} = \varepsilon_{ij}^{E} + \varepsilon_{ij}^{I} \tag{3.9}$$

Both components of the damage tensor $\boldsymbol{\varepsilon}^{ed}$ and $\boldsymbol{\varepsilon}^{id}$ are functions of an internal variable called the damage variable, ϕ, which is a scalar for isotropic damage and a tensor for a continuum that exhibits anisotropic damage. In the following section, we interpret the physical definition of the damage tensor in one-dimension and three-dimensions.

3.3 Physical Interpretation of the Damage Variable

The damage variable is a macroscopic measure of the microscopic degradation of a representative volume element (Kachanov, 1986; Lemaitre and Chaboche, 1990; Lemaitre; 1992; Lubarda and Krajcinovic, 1993; Voyiadjis and Venson, 1995; Krajcinovic, 1996; Voyiadjis and Kattan, 1999; Voyiadjis and Deliktas, 2000). Damage in materials can be represented in many forms such as specific void and crack surfaces, specific crack and void volumes, the spacing between cracks or voids, scalar representation of damage, and general tensorial representation of damage. In this section, however, the physical interpretation of the damage variable is introduced as the specific damaged surface area, where two cases are considered: the isotropic damage distribution case and the anisotropic damage distribution case of microcracks and microvoids. Moreover, this study is limited to small strain deformations and an extension to finite strain deformations can be easily obtained.

3.3.1 Isotropic Damage

We first consider the definition of the damage variable ϕ in one-dimension as originally proposed by Kachanov (1958), and further developed by several other authors (e.g. Lemaitre and Chaboche, 1990; Lemaitre; 1992; Lubarda and Krajcinovic, 1993; Voyiadjis and Venson, 1995; Krajcinovic, 1996; Voyiadjis and Kattan, 1999; Kattan and Voyiadjis, 2001) since the 1970s. Consider a uniform bar subjected to a uniaxial tensile load, T, as shown in Figure 3.4(a). The cross-sectional area of the bar in the stressed configuration is A and it is assumed that both voids and cracks appear as damage in the bar and form a total damage area of A^D. The uniaxial tensile force T acting on the bar is easily expressed using the formula $T = \sigma A$. In order to use the principles of continuum damage mechanics, one considers a fictitious undamaged configuration (effective configuration) of the bar as shown in Figure 3.4(b). In this configuration all types of damage, including both voids and cracks, are removed from the bar. The effective stressed cross-sectional area of the bar in this configuration is denoted by $\overline{A}$ and the effective uniaxial stress is $\overline{\sigma}$. The bars in both the damaged configuration and the effective undamaged configuration are subjected to the same tensile force, T. Therefore, considering the effective undamaged configuration, one can write $T = \overline{\sigma}\overline{A}$. Equating the two expressions for T that are obtained from both configurations, the following expression for the effective uniaxial stress $\overline{\sigma}$ (Kachanov, 1958; and Rabotnov, 1968) is derived such that:

$$\overline{\sigma} = \frac{\sigma}{1-\phi} \tag{3.10}$$

where

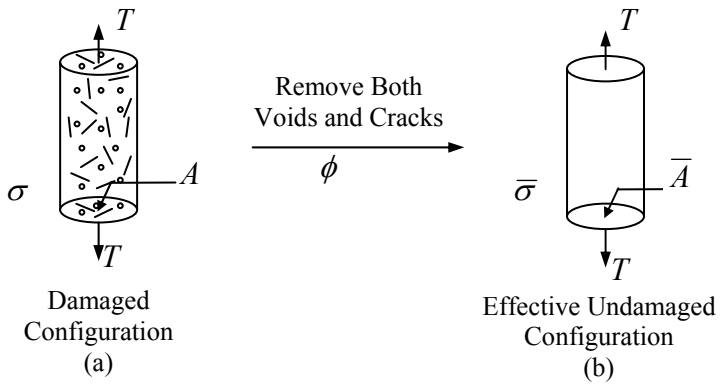

Figure 3.4 A cylindrical bar subjected to uniaxial tension: both voids and cracks are removed simultaneously (Voyiadjis and Kattan, 1999; Kattan and Voyiadjis, 2001).

$$\phi = \frac{A - \overline{A}}{A} = \frac{A^D}{A} \tag{3.11}$$

where A^D is the specific flaws (or damaged) area (Voyiadjis and Kattan, 1999; Kattan and Voyiadjis, 2001).

Similarly, a relation between the effective stress tensor, $\bar{\boldsymbol{\sigma}}$, and the nominal stress tensor, $\boldsymbol{\sigma}$, for the case of isotropic damage (i.e. scalar damage variable) can be written as follows:

$$\bar{\sigma}_{ij} = \frac{\sigma_{ij}}{1 - \phi} \tag{3.12}$$

One can now derive expressions for the elastic strains and elastic moduli in the damage configuration as a function of the isotropic damage variable ϕ. Assume that the initiated microcracks (no microvoids are initiated) during elastic loading are totally closed (not healed) upon the elastic unloading process. Figure 3.5(a) shows a fictitious stress-strain response before plasticity occurs, where the total elastic strain ($\boldsymbol{\varepsilon}^E = \boldsymbol{\varepsilon}^e + \boldsymbol{\varepsilon}^{ed}$) is recoverable. Thus, the elastic stress-strain relation can be written as:

$$\sigma_{ij} = \bar{E}_{ijkl} \varepsilon^e_{kl} \tag{3.13}$$

where $\bar{\boldsymbol{E}}$ is the initial elastic moduli that is constant and can be obtained experimentally.

The above equation shows that the initial elastic modulus, $\boldsymbol{E}$, is equal to the effective elastic modulus, $\bar{\boldsymbol{E}}$, if no damage occurs (i.e. $E = \bar{E}$ for no damage case). This is true if initially the current state has no micro-damage initiation. Thus, in this case the spatial configuration coincides with the effective fictitious configuration. Alternatively, Eq. (3.13) can also be written as follows (Figure 3.5(a)):

$$\sigma_{ij} = E_{ijkl} \left(\varepsilon^e_{kl} + \varepsilon^{ed}_{kl} \right) = E_{ijkl} \varepsilon^E_{kl} \tag{3.14}$$

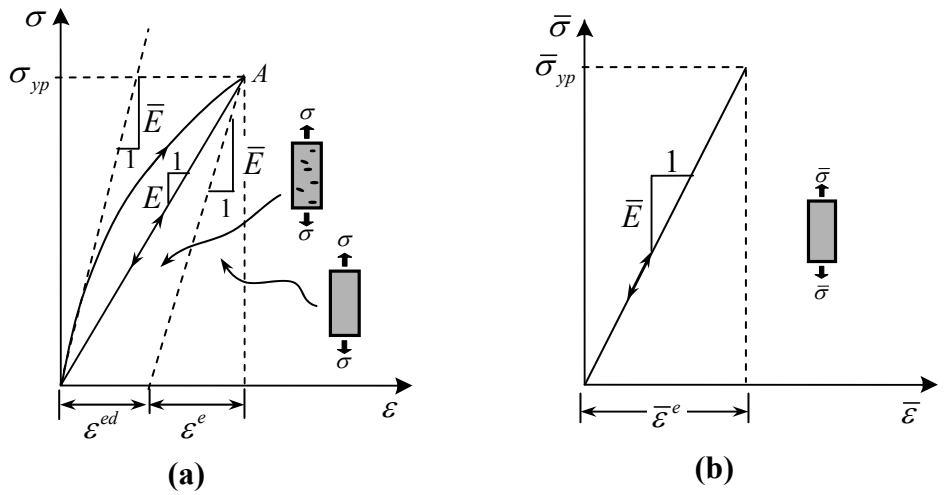

Figure 3.5 Fictitious uniaxial stress-strain elastic response where all the damage strain is recoverable.
(a) all damage is recoverable (all cracks are closed but not healed)
(b) effective configuration where all damage is removed.

where $\boldsymbol{E}$ is the elastic-damage Young's modulus (degraded) that is no longer constant, and hence a relation between the elastic-damage modulus $\boldsymbol{E}$ and the damage variable ϕ is sought.

Considering the fictitious effective (undamaged) stress-strain response shown in Figure 3.5(b), a similar relation to Eq. (3.13) can be obtained such as:

$$\bar{\sigma}_{ij} = \bar{E}_{ijkl}\bar{\varepsilon}^{e}_{kl} \tag{3.15}$$

where $\bar{\boldsymbol{\varepsilon}}^{e}$ and $\bar{\boldsymbol{E}}$ are the effective counterparts of $\boldsymbol{\varepsilon}^{E}$ and $\boldsymbol{E}$, respectively.

In order to derive the transformation relations between the damaged and the hypothetical undamaged (effective configuration) states of the material, the elastic energy equivalence hypothesis (Sidoroff, 1981) is utilized. This hypothesis assumes that the elastic energy in terms of effective and nominal stress and corresponding strain quantities must be equal. Thus, the elastic strain energy is equated to the effective elastic strain energy such that:

$$\frac{1}{2}\sigma_{ij}\,\varepsilon^{E}_{ij} = \frac{1}{2}\bar{\sigma}_{ij}\;\bar{\varepsilon}^{e}_{ij} \tag{3.16}$$

where $\boldsymbol{\varepsilon}^{E} = \boldsymbol{\varepsilon}^{e} + \boldsymbol{\varepsilon}^{ed}$ is the total elastic strain recovered during unloading and $\bar{\boldsymbol{\varepsilon}}^{e}$ is the effective elastic strain. The total elastic strain energy is assumed to be a decomposition of two parts: the ordinary elastic strain energy ($\frac{1}{2}\boldsymbol{\sigma}\,\boldsymbol{\varepsilon}^{e}$) and the elastic-damage strain energy ($\frac{1}{2}\boldsymbol{\sigma}\,\boldsymbol{\varepsilon}^{E} - \frac{1}{2}\boldsymbol{\sigma}\,\boldsymbol{\varepsilon}^{e}$). This signifies that the stored elastic-damage energy is needed to open the closed cracks during the elastic loading.

Substituting Eq. (3.12) into Eq. (3.16), the following relation between the effective elastic strain, $\bar{\boldsymbol{\varepsilon}}^e$, and the total elastic strain, $\boldsymbol{\varepsilon}^E$, is obtained as follows:

$$\bar{\varepsilon}_{ij}^e = (1-\phi)\,\varepsilon_{ij}^E \tag{3.17}$$

This is analogous to the relation derived by Voyiadjis and Kattan (1992a). However, in that work the strain $\boldsymbol{\varepsilon}^E$ was not explicitly decomposed into its components $\boldsymbol{\varepsilon}^e$ and $\boldsymbol{\varepsilon}^{ed}$.

A similar relation between the ordinary elastic strain, $\boldsymbol{\varepsilon}^e$, and the effective elastic strain, $\bar{\boldsymbol{\varepsilon}}^e$, can be obtained by substituting Eqs. (3.12) and (3.13) into Eq. (3.15) such that:

$$\varepsilon_{ij}^e = (1-\phi)\,\bar{\varepsilon}_{ij}^e \tag{3.18}$$

From the above relation it is clear that the effective elastic strain, $\bar{\boldsymbol{\varepsilon}}^e$, is not identical to the ordinary elastic strain, $\boldsymbol{\varepsilon}^e$, obtained through the additive strain decomposition in Eq. (3.7). This relation shows that the elastic strain (excluding the damage strain) depends on the damage level, which conforms well to the experimental observations that show the elastic strain decreases as the damage level increases, in particular, at strains close to failure, see Figure 3.6.

Furthermore, by rearranging Eq. (3.17) and substituting into Eq. (3.18) one obtains:

$$\varepsilon_{ij}^e = (1-\phi)^2\,\varepsilon_{ij}^E \tag{3.19}$$

which again emphasizes the previous result, see Figure 3.6. Considering the additive decomposition of the total elastic strain, Eq. (3.7), into Eq. (3.19) and simplifying the result we obtain a relation for the elastic-damage strain, $\boldsymbol{\varepsilon}^{ed}$, as follows:

$$\varepsilon_{ij}^{ed} = \left[\frac{1-(1-\phi)^2}{(1-\phi)^2}\right]\varepsilon_{ij}^e \tag{3.20}$$

or by utilizing Eqs. (3.18) and (3.19) one obtains the following relation:

$$\varepsilon_{ij}^{ed} = \left[\frac{1-(1-\phi)^2}{(1-\phi)}\right]\bar{\varepsilon}_{ij}^e = \left[1-(1-\phi)^2\right]\varepsilon_{ij}^E \tag{3.21}$$

This relation shows that the elastic-damage strain, $\boldsymbol{\varepsilon}^{ed}$, increases with the damage growth (Figures 3.6 and 3.7), which qualitatively agrees with the loading-unloading uniaxial tensile processes.

Finally, by substituting Eqs. (3.10) and (3.17) into Eq. (3.15) and comparing the result with Eq. (3.14), one derives a relation between the elastic-damage modulus, $\boldsymbol{E}$, and the initial elastic modulus, $\bar{\boldsymbol{E}}$, in terms of the scalar damage variable, ϕ, as follows:

$$E_{ijkl} = \bar{E}_{ijkl}\left(1-\phi\right)^2 \tag{3.22}$$

This coincides with the relation obtained by Voyiadjis and Kattan (1992a).

In Figure 3.6(a) the variation of the strain ratios in the elastic range of Eqs. (3.17), (3.19), and (3.21) are plotted with respect to the damage variable, ϕ. In Figure 3.6(b) the variation of

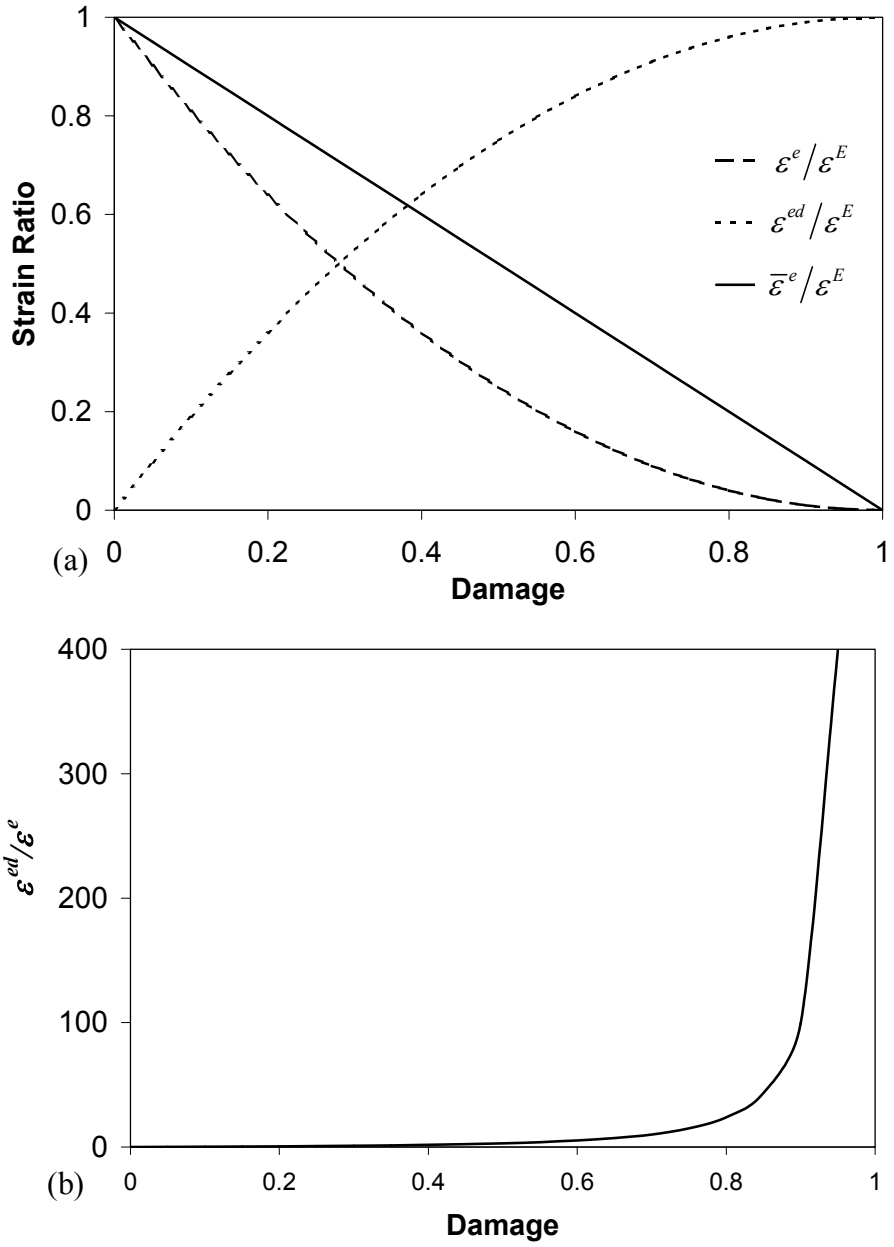

Figure 3.6 Variation of the different types of elastic strain with respect to the damage variable, ϕ. (a) with respect to the total elastic strain, (b) the elastic-damage strain to elastic strain ratio.

the strain ratio in the elastic range of Eq. (3.20) is plotted with respect to the damage variable, ϕ. Figure 3.6 shows a qualitatively correct behavior with respect to the experimental observations.

It is noteworthy that if the damage variable, ϕ, is known, one can then calculate the corresponding damage strain and stiffness using the derived equations. Next, we will demonstrate the proposed damage concept for the anisotropic case.

3.3.2 Anisotropic Damage

Many researchers tend to adopt the traditional simple isotropic scalar damage variable, "$(1-\phi)$", in order to model the material micro-damage mechanism, in which all components of the material stiffness are degraded by the same scalar damage parameter, ϕ (e.g. Krajcinovic and Foneska, 1981; Krajcinovic, 1983; Kachanov, 1986; Lemaitre and Chaboche, 1990; Lemaitre; 1992; Doghri, 2000; etc). However, in order to ensure a more realistic application of the principles of the damage mechanics, anisotropic damage should be assumed. In this case different levels of damage are related to the principal directions, and thus a simple scalar damage parameter is no longer sufficient to quantify damage in all directions. Instead, the anisotropic phenomenon of the microdamage distribution in the material is interpreted using a symmetric second-order damage tensor, ϕ_{ij} (e.g. Murakani and Ohno, 1981; Murakami, 1983, 1988; Ortiz, 1985; Chow and Wang, 1987, 1988; Lubarda and Krajcinovic, 1993; Voyiadjis and Abu-Lebdeh, 1993; Voyiadjis and Kattan, 1992a, 1992b; Voyiadjis and Venson, 1995; Voyiadjis and Park, 1997, 1999; Seweryn and Mroz, 1998; Voyiadjis and Deliktas, 2000; etc.).

We now generalize the definition of the isotropic damage variable described above (Figure 3.4) to the anisotropic case. Consider a damaged solid in which an RVE of finite volume has been isolated. Assume the RVE is an elementary parallelepiped, and consider facets of outward unit normal n_i $(i = x, y, z)$. Each of the three facets has a different evolution of microdamage; i.e. A_x^D on the facet has a unit normal n_x, A_y^D on the facet that has a unit normal n_y, and A_z^D on the facet that has a unit normal n_z. The total area of the facet in the n_x, n_y, and n_z directions are designated as A_x, A_y, A_z, respectively. A measure of damage in the RVE is then given by a second-order tensor defined as follows:

$$\boldsymbol{\phi} = \sqrt{\boldsymbol{\rho} \otimes \boldsymbol{\rho}} \qquad \text{or} \qquad \phi_{ij} = \sqrt{\rho_i \, \rho_j} \tag{3.23}$$

where $\boldsymbol{\rho}$ is the microdamage (microcracks and microvoids) density, and defined as follows:

$$\rho_i = \frac{A_i^D}{A_i} \qquad \text{(no sum on } i\text{)} \tag{3.24}$$

where A_i^D $(i = x, y, z)$ is the total area of defects traces on the facet whose unit normal is n_i. We will see in the subsequent sections that the definition of the strain energy release rate

enables us to avoid calculation of A_i^D which would be extremely difficult to do because of the lack of knowledge of the precise geometry of the microcracks and microvoids. A compound definition for damage was previously defined by Kattan and Voyiadjis (2001) were both damages due to cracks and voids were superimposed. Their definition of voids followed the concept of area reduction due to damage.

The damage tensor $\boldsymbol{\phi}$ in Eq. (3.23) can be written in a matrix form as follows:

$$[\phi] = \begin{bmatrix} \phi_{xx} & \phi_{xy} & \phi_{xz} \\ \phi_{yx} & \phi_{yy} & \phi_{yz} \\ \phi_{zx} & \phi_{zy} & \phi_{zz} \end{bmatrix} = \begin{bmatrix} \rho_x & \sqrt{\rho_x \rho_y} & \sqrt{\rho_x \rho_z} \\ \sqrt{\rho_y \rho_x} & \rho_y & \sqrt{\rho_y \rho_z} \\ \sqrt{\rho_z \rho_x} & \sqrt{\rho_z \rho_y} & \rho_z \end{bmatrix} \tag{3.25}$$

which is a generalization of the Kachanov's parameter that has in some simple special cases the same meaning. In the work of Voyiadjis and Venson (1995) crack densities as a measure of microcracks only without microvoids was considered. In a later work by Voyiadjis and Kattan (1999), and Kattan and Voyiadjis (2001) the two types of damages were incorporated under the same variable, ϕ. In the present work all the defect traces that evolve on the RVE facets (i.e. microcracks and microvoids) are considered.

It is worth to say that the above definition is defined from a pure geometric point of view; that is the larger the surface damage traces, the more severe the damage. From the material point of view, the distribution (spacing and orientation) and size of the surface damage traces have a considerable influence on the material behavior. For example the same total damaged area can be contributed by a smaller number of large voids/cracks or a larger number of small voids/cracks. Those effects are implicitly considered in the evolution equations derived in the subsequent sections. This implicit consideration comes from the fact that the proposed model follows the phenomenological approach because the material behavior is described through a suitable set of internal variables, acting at the micro-structural level, and whose relation to micromechanical processes is not exactly defined. However, an explicit consideration of such effects can be achieved by the use of the non-local or gradient damage theories (e.g. Pijaudier-Cabot and Bazant, 1987; Aifantis, 1992; Zbib and Aifantis, 1992; Voyiadjis et al., 2001, 2003; Voyiadjis and Abu Al-Rub, 2003; Taylor et al., 2002). This explicit consideration of the shape, size, and distribution of micro-cracks and micro-voids by the use of the non-local or gradient theories can be easily adapted to the proposed model, but the matter is beyond the scope and the limit of the present work.

One can write the linear elastic constitutive equations for the damaged material according to the principle of strain energy equivalence between the virgin material and damaged material (Sidoroff, 1981). That is, the damaged material is modeled using the constitutive laws of the effective undamaged material in which the Cauchy stress tensor, $\boldsymbol{\sigma}$, is replaced by the effective stress tensor, $\bar{\boldsymbol{\sigma}}$ (Murakani and Ohno, 1981):

$$\bar{\sigma}_{ij} = M_{ikjl}\sigma_{kl} \tag{3.26}$$

where $\boldsymbol{M}$ is the fourth-order damage-effect tensor. Many different expressions for $\boldsymbol{M}$ have been proposed in the literature in order to symmetrize the effective stress tensor, $\bar{\boldsymbol{\sigma}}$. A

comprehensive review of the most widely used expressions are presented by Voyiadjis and Park (1997). The following expression for $\boldsymbol{M}$, which is proposed by Cordebois and Sidoroff (1979), is used here due to its attractiveness in the mathematical formulations, such that:

$$M_{ikjl} = 2\left[\left(\delta_{ik} - \phi_{ik}\right)\delta_{jl} + \delta_{ik}\left(\delta_{jl} - \phi_{jl}\right)\right]^{-1} \tag{3.27}$$

where δ_{ij} is the Kronecker delta.

Furthermore, using the strain energy equivalence principle, Eq. (3.17) which relates the effective elastic strain tensor $\bar{\boldsymbol{\varepsilon}}^{e}$ with the total elastic strain tensor $\boldsymbol{\varepsilon}^{E}$ can be expressed for anisotropic damage as follows:

$$\bar{\varepsilon}_{ij}^{e} = M_{ikjl}^{-1}\varepsilon_{kl}^{E} \tag{3.28}$$

Also similar to Eq. (3.18), one can write:

$$\bar{\varepsilon}_{ij}^{e} = M_{ikjl}\varepsilon_{kl}^{e} \tag{3.29}$$

Analogous to Eq. (3.22), the elastic-damage stiffness, $\boldsymbol{E}$**,** can be rewritten using the fourth order damage-effect tensor $\boldsymbol{M}$ as follows (Voyiadjis and Park, 1999):

$$E_{ijkl} = M_{imjn}^{-1}\bar{E}_{mnpq}M_{pkql}^{-1} \tag{3.30}$$

where

$$M_{ikjl}^{-1} = \frac{1}{2}\left[\left(\delta_{ik} - \phi_{ik}\right)\delta_{jl} + \delta_{ik}\left(\delta_{jl} - \phi_{jl}\right)\right] \tag{3.31}$$

and $\bar{\boldsymbol{E}}$ is the fourth-order elastic moduli tensor given by:

$$\bar{E}_{ijkl} = \bar{K}\delta_{ij}\delta_{kl} + 2\bar{G}\left(\delta_{ik}\delta_{jl} - \frac{1}{3}\delta_{ij}\delta_{kl}\right) \tag{3.32}$$

where $\bar{K}$ and $\bar{G}$ are the elastic bulk and shear moduli, respectively.

Analogous to Eq. (3.21) one can express $\boldsymbol{\varepsilon}^{ed}$ in terms of the applied stress, $\boldsymbol{\sigma}$, by substituting Eqs. (3.13) and (3.14) into Eq. (3.7), such that:

$$\varepsilon_{ij}^{ed} = \left(E_{ijkl}^{-1} - \bar{E}_{ijkl}^{-1}\right)\sigma_{kl} \tag{3.33}$$

where $\boldsymbol{E}^{-1}$ and $\bar{\boldsymbol{E}}^{-1}$ are the inverse counterparts of Eqs. (3.30) and (3.32), respectively.

3.3.3 The Strain Energy Release Rate ($\mathcal{G}$)

The strain energy release rate $\mathcal{G}$ for the isotropic damage case is defined as the rate of change in the elastic potential energy density $\bar{\Psi}^E$ with respect to the specific damaged area A^D for a linear elastic material, such that:

$$\mathcal{G} = -\frac{\partial \bar{\Psi}^E}{\partial A^D} \tag{3.34}$$

Now, we illustrate the derivation of the strain energy release rate $\mathcal{G}$ in one dimension. Consider an elastically loaded body containing microdamages (Figure 3.5). The potential energy $\bar{\Psi}^E$ for damage growth is given by:

$$\bar{\Psi}^E = U - W \tag{3.35}$$

where U is the strain energy stored in the body ($\sigma\varepsilon^E/2$) and W is the additional energy necessary for damage growth and obtained from the work done by $\sigma\varepsilon^E$. The potential energy $\bar{\Psi}^E$, therefore, can be written as follows:

$$\bar{\Psi}^E = -\frac{1}{2}\sigma\varepsilon^E \tag{3.36}$$

Eq. (3.36) is obtained when the loading is stress controlled (the displacement is fixed). However, if the loading is strain controlled (the load is fixed), the potential energy $\bar{\Psi}^E$ is given as:

$$\bar{\Psi}^E = \frac{1}{2}\sigma\varepsilon^E \tag{3.37}$$

Now substitution of Eq. (3.37) into Eq. (3.34) along with $\varepsilon^E = \sigma/E$, yields the following expression:

$$\mathcal{G} = -\frac{1}{2}\left[\frac{2\sigma}{E}\frac{\partial\sigma}{\partial A^D} + \sigma^2\frac{\partial}{\partial A^D}\left(\frac{1}{E}\right)\right] \tag{3.38}$$

The stiffness of the body E is decreasing whether the body is rigidly gripped (strain control) such that the damage growth would result in a stress drop or whether the stress is fixed (stress control) such that the damage growth would result in a strain increase. For the strain control case, both σ and E would decrease, but the ratio σ/E would remain the same, such that:

$$\frac{1}{E}\frac{\partial\sigma}{\partial A^D} + \sigma\frac{\partial}{\partial A^D}\left(\frac{1}{E}\right) = 0 \tag{3.39}$$

Using the above equation with Eq. (3.38), the following expression is obtained for $\mathcal{G}$, such that:

$$\mathcal{G} = \frac{1}{2}\sigma^2 \frac{\partial}{\partial A^D}\left(\frac{1}{E}\right) \tag{3.40}$$

In the case of stress control or strain control loading, the magnitude of $\bar{\Psi}^E$ is equivalent as given by Eqs. (3.36) and (3.37). Thus, under fixed stress loading condition the strain energy release rate is the same as given by Eq. (3.40), only the sign is reversed, reflecting the fact the $\mathcal{G}$ is independent of the type of load application (e.g. displacement control, load control, combinations of stress change and strain change).

We found for the case of isotropic damage (Eq. (3.22)) that E for a one-dimensional case can be expressed in terms of the undamaged stiffness $\bar{E}$ and the damage variable ϕ as follows:

$$E = \bar{E}\left(1-\phi\right)^2 \tag{3.41}$$

with $\phi = A^D / A$ is given by Eq. (3.11).

Substitution of Eq. (3.41) into Eq. (3.40), yields the following expression for the energy release rate $\mathcal{G}$:

$$\mathcal{G} = \frac{\sigma^2}{A\bar{E}\left(1-\phi\right)^3} \tag{3.42}$$

By substituting the nominal stress σ from Eq. (3.10) along with the elastic strain energy equivalence principle (Eq. (3.16)), the strain energy release rate $\mathcal{G}$ can be written as a function of the energy potential and the damage variable as follows:

$$\mathcal{G} = \frac{2\bar{\Psi}^E}{A\left(1-\phi\right)} \tag{3.43}$$

The strain energy release rate for the anisotropic damage can be defined as follows:

$$\mathcal{G}_{ij} = -\frac{\partial \bar{\Psi}^E}{\partial A^D_{ij}} \tag{3.44}$$

where $A^D_{ij} = A^D_i A^D_j$ as defined in Eq. (3.23).

Similar to the procedure outlined above, one can derive the strain energy release rate for the anisotropic damage case ($\boldsymbol{\mathcal{G}}$) with the aid of the definition presented by Eqs. (3.23), (3.30)

and (3.31). Assuming that the total area of the RVE's facets in the n_x, n_y, and n_z normals are constant, one can write $\mathcal{G}$ as follows:

$$\mathcal{G}_{ij} = 2\bar{\Psi}^E M_{kplq} \frac{\partial M^{-1}_{kplq}}{\partial \phi_{ab}} \frac{\partial \phi_{ab}}{\partial A^D_{ij}} \tag{3.45}$$

Using Eq. (3.27), one can write:

$$\frac{\partial M^{-1}_{kplq}}{\partial \phi_{ab}} = -J_{kplqab} \tag{3.46}$$

where $\boldsymbol{J}$ is a sixth-order tensor and is given by:

$$J_{kplqab} = \frac{1}{2}\left(\delta_{lq}\delta_{ka}\delta_{pb} + \delta_{kp}\delta_{la}\delta_{qb}\right) \tag{3.47}$$

Hence, Eq. (3.45) can be written as:

$$\mathcal{G}_{ij} = -2\bar{\Psi}^E M_{kplq} J_{kplqab} \frac{\partial \phi_{ab}}{\partial A^D_{ij}} \tag{3.48}$$

where $\bar{\Psi}^E$ is given by:

$$\bar{\Psi}^E = \frac{1}{2}\bar{\sigma}_{ij}\bar{E}^{-1}_{ijkl}\bar{\sigma}_{kl} = \frac{1}{2}\sigma_{ij}E^{-1}_{ijkl}\sigma_{kl} \tag{3.49}$$

It is noteworthy that since the magnitude of $\bar{\Psi}^E$ is path independent as was shown in the beginning of this section, the expression of $\mathcal{G}$ does not differ whether the imposed loading is strain control or stress control. This particularly agrees well with the definition of strain energy release rate made in fracture mechanics (Thomason, 1990; Anderson; 1994; Hertzberg, 1996). However, this does not imply that the strain energy release rate, presented in Eq. (3.43) for isotropic damage or Eq. (3.48) for anisotropic damage, is stress/force path independent. The expression for the strain energy release rate, which is used later to define the conjugate damage force, has in its composition the damage variable $\boldsymbol{\phi}$ which is stress/force path dependent. This makes both the strain energy release rate and the damage conjugate force path dependent.

3.4 Coupled Damage/Plasticity Thermodynamic Formulation

3.4.1 Helmholtz Free Energy Density

In this work, the elasto-plastic-damage material behavior is considered. This implies that stress path material dependence and the nonlinear material response are considered. Thus, the dependent constitutive variables are functions of the total elastic strain tensor, $\boldsymbol{\varepsilon}^E$, and n_{int} - of

internal state variables, $\aleph_k$ ($k = 1,...,n_{\text{int}};\ n_{\text{int}} \geq 1$). Within the thermodynamic framework, the Helmholtz free energy density can be written as:

$$\Psi = \Psi\left(\varepsilon_{ij}^{E}; \aleph_k\right) \tag{3.50}$$

Since the main objective is to develop strong-coupled constitutive equations for a plastic-damaged material, the effects of plastic strain hardening and micro-damage mechanisms are to be considered. Experimental observations show that the accumulation of the material defects during the deformation process has a tendency to form macroscopically localized deformation regions. In those localized zones, many defects may undergo irreversible growth; coalescence of pre-existing cracks and voids may occur; propagation of dislocations may proceed; and new defects may nucleate with their ultimate coalescence results in failure. Moreover, intensive interaction mechanisms of the evolved defects may take place at those localized zones; such as dislocation - dislocation interaction, microdamage - microdamage interaction, crack dominated - dislocation interaction, dislocation dominated - crack interaction, dislocation/crack - grain boundary interaction, etc. In order to consider such mechanisms in the constitutive equations, a finite set of internal state variables $\aleph_k$, acting at the micro-structural level, representing either a scalar or a tensorial variable are assumed such that (Voyiadjis and Deliktas, 2000):

$$\aleph_k = \aleph_k\left(\alpha_{ij}, p, \Gamma_{ij}, r, \phi_{ij}\right) \tag{3.51}$$

where $\boldsymbol{\alpha}$ is the plastic flux variable related to the kinematic hardening (movement of the loading surface), and p is the equivalent plastic strain related to the isotropic hardening (size of the loading surface). Furthermore, since this work focuses on the development of a coupled plastic-damage framework based on the thermomechanical postulates, the various possibilities to describe anisotropic damage are to be presented here. The damage internal variables consist of the damage flux variable $\boldsymbol{\Gamma}$ corresponding to the kinematic hardening (movement of the damage surface), r the cumulative inelastic-damage strain (size of the damage surface), and $\boldsymbol{\phi}$ the anisotropic damage tensor. p and r can be expressed as follows:

$$p = \int_0^t \sqrt{\tfrac{3}{2}\dot{\varepsilon}_{ij}^{p}\dot{\varepsilon}_{ij}^{p}}\, dt \tag{3.52}$$

$$r = \int_0^t \sqrt{\dot{\varepsilon}_{ij}^{id}\dot{\varepsilon}_{ij}^{id}}\, dt \tag{3.53}$$

Using the Clausius-Duhem inequality for isothermal state, one obtains:

$$\sigma_{ij}\dot{\varepsilon}_{ij} - \rho\dot{\psi} \geq 0 \tag{3.54}$$

where ρ denotes the mass density. In Eq. (3.54) the total strain rate tensor, $\dot{\boldsymbol{\varepsilon}}$, is decomposed into two parts: total elastic part, $\dot{\boldsymbol{\varepsilon}}^{E} = \dot{\boldsymbol{\varepsilon}}^{e} + \dot{\boldsymbol{\varepsilon}}^{ed}$ and inelastic part, $\dot{\boldsymbol{\varepsilon}}^{I} = \dot{\boldsymbol{\varepsilon}}^{p} + \dot{\boldsymbol{\varepsilon}}^{id}$.

The time derivative of Eq. (3.50) with the respect to its internal state variables, $\aleph_k$, is given by:

$$\dot{\Psi} = \frac{\partial \Psi}{\partial \varepsilon_{ij}^E} \dot{\varepsilon}_{ij}^E + \frac{\partial \Psi}{\partial \alpha_{ij}} \dot{\alpha}_{ij} + \frac{\partial \Psi}{\partial p} \dot{p} + \frac{\partial \Psi}{\partial \Gamma_{ij}} \dot{\Gamma}_{ij} + \frac{\partial \Psi}{\partial r} \dot{r} + \frac{\partial \Psi}{\partial \phi_{ij}} \dot{\phi}_{ij} \tag{3.55}$$

Substituting the rate of the Helmholtz free energy density, Eq. (3.55), into the Clausius-Duhem inequality, Eq. (3.54), along with Eq. (3.5), one obtains the following thermodynamic constraint:

$$\left(\sigma_{ij} - \rho \frac{\partial \Psi}{\partial \varepsilon_{ij}^E} \right) \dot{\varepsilon}_{ij}^E + \sigma_{ij} \dot{\varepsilon}_{ij}^I - \rho \frac{\partial \Psi}{\partial \alpha_{ij}} \dot{\alpha}_{ij} - \rho \frac{\partial \Psi}{\partial p} \dot{p} - \rho \frac{\partial \Psi}{\partial \Gamma_{ij}} \dot{\Gamma}_{ij} - \rho \frac{\partial \Psi}{\partial r} \dot{r} - \rho \frac{\partial \Psi}{\partial \phi_{ij}} \dot{\phi}_{ij} \geq 0 \tag{3.56}$$

Eq. (3.56) results in the following thermodynamic state laws for the conjugate thermodynamic forces:

$$\sigma_{ij} = \rho \frac{\partial \Psi}{\partial \varepsilon_{ij}^E} \tag{3.57}$$

$$X_{ij} = \rho \frac{\partial \Psi}{\partial \alpha_{ij}} \tag{3.58}$$

$$R = \rho \frac{\partial \Psi}{\partial p} \tag{3.59}$$

$$H_{ij} = \rho \frac{\partial \Psi}{\partial \Gamma_{ij}} \tag{3.60}$$

$$K = \rho \frac{\partial \Psi}{\partial r} \tag{3.61}$$

$$-Y_{ij} = \rho \frac{\partial \Psi}{\partial \phi_{ij}} \tag{3.62}$$

where $\boldsymbol{X}$, R, $\boldsymbol{H}$, K, and $\boldsymbol{-Y}$ are the thermodynamic forces conjugate to the fluxes $\boldsymbol{\alpha}$, p, $\boldsymbol{\Gamma}$, r, and $\boldsymbol{\phi}$, respectively.

The complexity of a model is directly determined by the form of the Helmholtz free energy Ψ and by the number of conjugate pairs of variables. The specific free energy, Ψ, on the long-term manifold (neglecting the short-term manifolds) is assumed as follows:

$$\rho\Psi = \frac{1}{2} \varepsilon_{ij}^E E_{ijkl}(\boldsymbol{\phi}) \varepsilon_{kl}^E + \frac{1}{3} C \alpha_{ij} \alpha_{ij} + Q\left(p + \frac{1}{b} e^{-bp} \right) + \frac{1}{2} a \Gamma_{ij} \Gamma_{ij} + q\left(r + \frac{1}{c} e^{-cr} \right) \tag{3.63}$$

where $\boldsymbol{E}(\boldsymbol{\phi})$ is the fourth-order damage elastic tensor and C, Q, b, a, and c are material-dependent constants.

The form of the first term in Eq. (3.63) has been often postulated in damage mechanics, and is based on the concept of the effective stress $\bar{\boldsymbol{\sigma}}$ so that it presents the same strain or the same elastic energy as a damaged element subjected to the nominal stress $\boldsymbol{\sigma}$. The rest of the terms in Eq. (3.63) have been assumed in this form in order to derive nonlinear evolution equations for the isotropic and kinematic hardening that describe more accurately the plasticity and damage deformation mechanisms. The second and third terms take a form as proposed by Chaboche (1989). The fourth and fifth terms are assumed analogous to the second and third terms, respectively for the case of damage.

The proposed definition of Ψ allows the derivation of the constitutive equations and the internal dissipation described next. The state laws of the assumed internal state variables are obtained by substituting Eq. (3.63) into Eqs. (3.57)-(3.61), such that:

$$\sigma_{ij} = E_{ijkl}\left(\varepsilon_{kl} - \varepsilon_{kl}^{p} - \varepsilon_{kl}^{id}\right) \tag{3.64}$$

$$X_{ij} = \frac{2}{3} C \alpha_{ij} \tag{3.65}$$

$$R = Q\left(1 - e^{-bp}\right) \tag{3.66}$$

$$H_{ij} = a\Gamma_{ij} \tag{3.67}$$

$$K = q\left(1 - e^{-cr}\right) \tag{3.68}$$

Now, one can obtain an expression for the damage driving force $\boldsymbol{Y}$ in terms of the strain energy release rate presented in Eq. (3.45). By using the chain rule, the thermodynamic state law of $\boldsymbol{Y}$ (Eq. (3.62)) can be written as follows:

$$Y_{ij} = -\rho \frac{\partial \Psi^{E}}{\partial A_{mn}^{D}} \frac{\partial A_{mn}^{D}}{\partial \phi_{ij}} \tag{3.69}$$

Using the definition of strain energy release rate for anisotropic damage (Eq. (3.44)) and the physical definition of the damage tensor $\boldsymbol{\phi}$ (Eqs. (3.23) and (3.24)) along with the assumption of A designating the total area of the RVE's facets in the n_x, n_y, and n_z directions, one can write Eq. (3.69) in terms of the strain release rate, $\mathcal{G}$, as follows:

$$Y_{ij} = \mathcal{G}_{mn} \frac{\partial A_{mn}^{D}}{\partial \phi_{ij}} \tag{3.70}$$

Substituting the expression derived for the strain energy release rate for anisotropic damage $\mathcal{G}$ (Eq. (3.48)) into Eq. (3.70), one can express the damage driving force $\boldsymbol{Y}$ as follows:

$$Y_{ij} = 2\bar{\Psi}^{E} M_{kplq} J_{kplqij} \tag{3.71}$$

where $\bar{\Psi}^E$ and $\boldsymbol{J}$ are given by Eqs. (3.47) and (3.49), respectively. Furthermore, we may replace $\bar{\Psi}^E = \boldsymbol{\sigma} : \bar{\boldsymbol{\varepsilon}}^e / 2$ by its expression in terms of equivalent stress $\bar{\sigma}_{eq} = \sqrt{3\bar{\boldsymbol{\tau}} : \bar{\boldsymbol{\tau}} / 2}$ and the hydrostatic stress $\bar{P} = trac(\bar{\boldsymbol{\sigma}}) / 3$ as follows:

$$\bar{\Psi}^E = \frac{\bar{\sigma}_{eq}^2}{6\bar{G}} + \frac{9\bar{P}^2}{2\bar{K}} \tag{3.72}$$

where $\bar{K} = 3\bar{E}/(1-2\bar{\nu})$, $\bar{G} = \bar{E}/2(1+\bar{\nu})$, and $\bar{\nu}$ is the Poisson's ratio. For the isotropic damage case we may write an expression for Y as follows:

$$Y = \frac{\bar{\sigma}^{*2}}{\bar{E}(1-\phi)} = \frac{\sigma^{*2}}{E(1-\phi)} \tag{3.73}$$

with

$$\bar{\sigma}^* = \bar{\sigma}_{eq}[\tfrac{2}{3}(1+\bar{\nu}) + 3(1-2\bar{\nu})(\bar{P}/\bar{\sigma}_{eq})^2]^{1/2} \tag{3.74}$$

where $\sigma^* = (1-\phi)\bar{\sigma}^*$. This is referred to as the equivalent damage stress according to the notation by Lemaitre and Chaboche (1990). The ratio $\bar{P}/\bar{\sigma}_{eq}$ expresses the triaxiality of the state of stress.

3.4.2 The Dissipation Function and the Maximum Dissipation Principle

Using the equations of state (Eqs. (3.57)-(3.62)), the Clausius-Duhem inequality expression (Eq. (3.56)) becomes:

$$\Pi = \sigma_{ij}\left(\dot{\varepsilon}_{ij}^p + \dot{\varepsilon}_{ij}^{id}\right) - X_{ij}\dot{\alpha}_{ij} - R\dot{p} - H_{ij}\dot{\Gamma}_{ij} - K\dot{r} + Y_{ij}\dot{\phi}_{ij} \geq 0 \tag{3.75}$$

where Π defines the dissipation due to plasticity and damage morphologies and requires to be non-negative. It can be seen from the dissipation function Π that both irreversible and reversible damage strains cause energy dissipation. This is caused by the irreversible strains through $\boldsymbol{\sigma} : \dot{\boldsymbol{\varepsilon}}^{id}$ and the reversible strains through $\boldsymbol{Y} : \dot{\boldsymbol{\phi}}$.

The rate of the internal state variables associated with plastic and damage deformations are obtained by utilizing the calculus of functions of several variables with the Lagrange multipliers $\dot{\lambda}^p$ and $\dot{\lambda}^d$, respectively. The dissipation function Π (Eq. (3.75)) is subjected to the two constraints, namely $f = 0$ and $g = 0$ (Voyiadjis and Kattan, 1992a), such that:

$$\Omega = \Pi - \dot{\lambda}^p f - \dot{\lambda}^d g \tag{3.76}$$

We now can make use of the maximum dissipation principle (Simo and Honein, 1990; Simo and Hughes, 1998), which states that the actual state of the thermodynamic forces ($\boldsymbol{\sigma}$, $\boldsymbol{Y}$) is

that which maximizes the dissipation function over all other possible admissible states. Thus, we maximize the objective function Ω by using the necessary conditions as follows:

$$\frac{\partial \Omega}{\partial \sigma_{ij}} = 0 \quad \text{and} \quad \frac{\partial \Omega}{\partial Y_{ij}} = 0 \tag{3.77}$$

Substitution of Eq. (3.76) into Eq. (3.77) along with Eq. (3.75) yields the thermodynamic laws corresponding to the evolution of the total inelastic strain rate ($\boldsymbol{\varepsilon}^I$) and the damage variable ($\boldsymbol{\phi}$), where Eq. $(3.77)_1$ gives the inelastic strain rate as follows:

$$\dot{\varepsilon}_{ij}^I = \dot{\lambda}^p \frac{\partial f}{\partial \sigma_{ij}} + \dot{\lambda}^d \frac{\partial g}{\partial \sigma_{ij}} \tag{3.78}$$

Considering the earlier postulate of the additive decomposition of the inelastic strain rate into plastic and damage parts, Eq. (3.8), the following assumption is made:

$$\dot{\varepsilon}_{ij}^p = \dot{\lambda}^p \frac{\partial f}{\partial \sigma_{ij}} \quad \text{and} \quad \dot{\varepsilon}_{ij}^{id} = \dot{\lambda}^d \frac{\partial g}{\partial \sigma_{ij}} \tag{3.79}$$

This assumption suggests that the inelastic-damage strains, $\boldsymbol{\varepsilon}^{id}$, may be anticipated even before any plastic deformation can be observed, which qualitatively meets the discussion outlined in Section 3.2.

On the other hand, Eq. $(3.77)_2$ gives the damage rate evolution law as follows:

$$\dot{\phi}_{ij} = \dot{\lambda}^p \frac{\partial f}{\partial Y_{ij}} + \dot{\lambda}^d \frac{\partial g}{\partial Y_{ij}} \tag{3.80}$$

Eq. (3.80) signifies, once again, that the damage growth occurs even if there is no plastic flow (i.e. $\dot{\lambda}^p = 0$), which agrees well with the experimental observations in brittle materials and is justified in Figure 3.5.

In order to obtain non-associative rules for the damage and plasticity hardening variables, one can assume the existence of a plastic potential F and a damage potential G such that they are respectively not equal to f and g. This postulate is essential in order to obtain nonlinear plastic and damage hardening rules, which give a more realistic characterization of the material response in the deformation process. The complementary laws for the evolution of the other internal state variables can then be obtained directly from the generalized normality rule, such that:

$$\dot{\alpha}_{ij} = -\dot{\lambda}^p \frac{\partial F}{\partial X_{ij}} \tag{3.81}$$

$$\dot{p} = -\dot{\lambda}^p \frac{\partial F}{\partial R} \tag{3.82}$$

$$\dot{\Gamma}_{ij} = -\dot{\lambda}^d \frac{\partial G}{\partial H_{ij}} \tag{3.83}$$

$$\dot{r} = -\dot{\lambda}^d \frac{\partial G}{\partial K} \tag{3.84}$$

where $\dot{\lambda}^p$ and $\dot{\lambda}^d$ are determined using the consistency conditions $\dot{f} = 0$ and $\dot{g} = 0$, respectively.

The next step is the selection of the appropriate form of the plastic potential function F, the plastic yield surface f, the damage potential function G, and the damage growth surface g in order to establish the desired constitutive equations that describe the mechanical behavior of the material.

3.4.3 Plasticity and Damage Dissipation Potentials and Hardening Rules

Plastic Dissipation Potential and Hardening Rules

Once a material is damaged, further loading can only affect the undamaged material. Thus, the damage potential function G is defined in terms of the effective stresses and strains. By combining plasticity with damage, it seems natural that plasticity can only affect the undamaged material skeleton. Thus plastic potential F is also defined in terms of the effective stresses and strains. The plastic potential F is defined as:

$$F = f + \frac{3}{4}\frac{\gamma}{C}\bar{\mathrm{X}}_{ij}\bar{\mathrm{X}}_{ij} \tag{3.85}$$

where γ and C are material constants used to adjust the units of the equation. The yield function, f, is of a von Mises type given as follows:

$$f = \sqrt{\tfrac{3}{2}(\bar{\tau}_{ij} - \bar{X}_{ij})(\bar{\tau}_{ij} - \bar{X}_{ij})} - \sigma_{yp} - \bar{R}(p) = 0 \tag{3.86}$$

where σ_{yp} is the initial size of the yield surface, and $\bar{\boldsymbol{\tau}}$ and $\bar{\boldsymbol{X}}$ are expressed in terms of the damage tensor $\boldsymbol{M}$ (given by Eq. (3.27)) and the corresponding damage states as follows (Voyiadjis and Kattan, 1999):

$$\bar{\tau}_{ij} = M'_{ikjl}\sigma_{kl} \quad \text{where} \quad M'_{ikjl} = M_{ikjl} - \frac{1}{3}M_{rkrl}\delta_{ij} \tag{3.87}$$

and

$$\bar{X}_{ij} = M_{ikjl}X_{kl} \tag{3.88}$$

The plastic parameter $\dot{\lambda}^p \geq 0$, which is known as the plastic consistency parameter, is assumed to obey the following Kuhn-Tucker loading/unloading conditions:

$$f \le 0 \text{ and } \dot{f} \begin{cases} < 0 & \Rightarrow \dot{\lambda}^{\mathrm{p}} = 0 \\ = 0 & \Rightarrow \dot{\lambda}^{\mathrm{p}} = 0 \\ = 0 & \Rightarrow \dot{\lambda}^{\mathrm{p}} > 0 \end{cases} \Leftrightarrow \begin{cases} \text{elastic unloading} \\ \text{neutral loading} \\ \text{plastic loading} \end{cases} \tag{3.89}$$

In order to derive the evolution of the plasticity isotropic hardening function, the time rate of Eq. (3.66) gives:

$$\dot{R} = bQ\dot{p}e^{-bp} \tag{3.90}$$

A relation between R and p can be obtained from Eq. (3.66), such that:

$$p = -\frac{1}{b}\ln\left(1 - \frac{R}{Q}\right) \tag{3.91}$$

which upon substituting it into Eq. (3.90) yields the following expression for $\dot{R}$, such that:

$$\dot{R} = b\left[Q - R\right]\dot{p} \tag{3.92}$$

The isotropic hardening represents a global expansion in the size of the yield surface with no change in shape. Thus for a given yield criterion and flow rule, isotropic hardening in any process can be predicted from the knowledge of the function $\bar{R}$, and this function may in principle, be determined from a single test (e.g. the tension test). Therefore, the effective isotropic hardening function $\bar{R}$ is related to the nominal isotropic hardening function by Eq. (3.10) as follows:

$$\bar{R} = \frac{R}{1 - \phi_{eq}} \tag{3.93}$$

where (Voyiadjis and Park, 1997)

$$\phi_{eq} = \sqrt{\phi_{ij}\phi_{ij}} \tag{3.94}$$

Using Eq. (3.82) along with the chain rule and Eqs. (3.86) and (3.93), it can be easily shown that $\dot{p}$ is related to $\dot{\lambda}^{p}$ by:

$$\dot{\lambda}^{p} = \left(1 - \phi_{eq}\right)\dot{p} \tag{3.95}$$

Using the chain rule and Eq. (3.88), Eq. (3.81) is now expressed as follows:

$$\dot{\alpha}_{ij} = -\dot{\lambda}^{p} M_{minj} \frac{\partial F}{\partial \bar{X}_{mn}} \tag{3.96}$$

Substitution of Eq. (3.85) into the above equation yields:

$$\dot{\alpha}_{ij} = -\dot{\lambda}^{p} M_{minj}\left(\frac{\partial f}{\partial \bar{X}_{mn}} + \frac{3}{2}\frac{\gamma}{C}\bar{X}_{mn}\right) \tag{3.97}$$

Since $\partial f/\partial \bar{\boldsymbol{X}} = -\partial f/\partial \bar{\boldsymbol{\sigma}}$ as it is clear from Eq. (3.86), it is easily shown with using the chain rule and Eqs. (3.26), $(3.79)_1$, (3.88) together with the time rate of Eq. (3.65) that the evolution equation of the plastic kinematic hardening $\dot{\boldsymbol{X}}$ is related to $\dot{\boldsymbol{\varepsilon}}^{p}$, $\boldsymbol{X}$, and $\boldsymbol{M}$ as follows:

$$\dot{X}_{ij} = \frac{2}{3}C\dot{\varepsilon}^{p}_{ij} - \gamma\dot{\lambda}^{p} M_{minj} M_{mrns} X_{rs} \tag{3.98}$$

Substituting Eq. (3.95) into the above equation, gives the following form for the evolution equation of the backstress tensor $\dot{\boldsymbol{X}}$, such that:

$$\dot{X}_{ij} = \frac{2}{3}C\dot{\varepsilon}^{p}_{ij} - \gamma\left(1-\phi_{eq}\right) M_{minj} M_{mrns} X_{rs}\dot{p} \tag{3.99}$$

Damage Dissipation Potential and Hardening Rules

The anisotropic damage governing equations are formulated using similar mathematical concepts as those used for plasticity. Thus, analogous to the plasticity potential function F, one can assume the following form of the damage potential function G in the space of the damage forces and the conjugated forces of the hardening variables (Voyiadjis and Deliktas, 2000):

$$G = g + \frac{1}{2}\frac{d}{a}H_{ij}H_{ij} \tag{3.100}$$

where d and a are material constants used to adjust the units of the equation. g is the damage growth function postulated as follows:

$$g = \sqrt{\left(Y_{ij} - H_{ij}\right)\left(Y_{ij} - H_{ij}\right)} - l_{d} - K\left(r\right) = 0 \tag{3.101}$$

where l_{d} is the initial damage threshold. The damage consistency parameter $\dot{\lambda}^{d} \geq 0$ is assumed to obey the following Kuhn-Tucker conditions:

$$g \leq 0 \text{ and } \dot{g}\begin{Bmatrix} < 0 \Rightarrow \dot{\lambda}^{\mathrm{d}} = 0 \\ = 0 \Rightarrow \dot{\lambda}^{\mathrm{d}} = 0 \\ = 0 \Rightarrow \dot{\lambda}^{\mathrm{d}} > 0 \end{Bmatrix} \Leftrightarrow \begin{cases} \text{undamaged state} \\ \text{damage initiation} \\ \text{damage growth} \end{cases} \tag{3.102}$$

Using Eq. (3.84) along with Eq. (3.101), the following relation is obtained:

$$\dot{\lambda}^{d} = \dot{r} \tag{3.103}$$

Taking the time rate of Eq. (3.68) and expressing r in terms of K, the evolution of the damage isotropic hardening function K can be easily written as:

$$\dot{K} = c\left(q - K\right)\dot{r} \tag{3.104}$$

Now, we derive an expression for the damage kinematic hardening rule by taking the time rate of Eq. (3.67) and making use of Eqs. (3.80), (3.83), (3.100), and (3.103) such that:

$$\dot{H}_{ij} = \left(a\frac{\partial g}{\partial Y_{ij}} - d\, H_{ij} \right)\dot{r} \tag{3.105}$$

where

$$\frac{\partial g}{\partial Y_{ij}} \equiv \frac{Y_{ij} - H_{ij}}{\sqrt{\left(Y_{kl} - H_{kl}\right)\left(Y_{kl} - H_{kl}\right)}} \tag{3.106}$$

Next, explicit expressions for the plasticity and damage Lagrange parameters $\dot{\lambda}^{p}$ and $\dot{\lambda}^{d}$ are derived using the consistency conditions $\dot{f}$ and $\dot{g}$, respectively.

3.4.4 Plasticity and Damage Consistency Conditions

Since $\bar{\boldsymbol{\sigma}}$, $\bar{\boldsymbol{X}}$, and $\bar{R}$ are functions of $\boldsymbol{\phi}$ and their corresponding nominal counter parts $\boldsymbol{\sigma}$, $\boldsymbol{X}$, and R, it follows that the yield function f may be expressed as a function $\boldsymbol{\phi}$, such that the corresponding consistency condition $\dot{f} = 0$ can be written as follows:

$$\dot{f} \equiv \frac{\partial f}{\partial \sigma_{ij}}\dot{\sigma}_{ij} + \frac{\partial f}{\partial X_{ij}}\dot{X}_{ij} + \frac{\partial f}{\partial R}\dot{R} + \frac{\partial f}{\partial \phi_{ij}}\dot{\phi}_{ij} = 0 \tag{3.107}$$

By assuming that the elastic-damage stiffness, $\boldsymbol{E}$, is constant within each stress/strain increment, which is the case in the strain-driven problem, one can write the time rate of the Cauchy stress tensor ($\dot{\boldsymbol{\sigma}}$) as follows:

$$\dot{\sigma}_{ij} = E_{ijkl}\dot{\varepsilon}^{E}_{kl} \tag{3.108}$$

Making use of the above equation, Eqs. (3.78), (3.80), (3.86), (3.92), (3.93), (3.95), (3.99), and the chain rule while noting that $\partial f/\partial \boldsymbol{X} = -\partial f/\partial \boldsymbol{\sigma}$, it can be shown, after some manipulation, that the consistency condition, Eq. (3.107), gives the following relation between $\dot{\lambda}^{p}$ and $\dot{\lambda}^{d}$, such that:

$$a_{11}\dot{\lambda}^{p} + a_{12}\dot{\lambda}^{d} = b_1 \tag{3.109}$$

where

$$a_{11} = \frac{\partial f}{\partial \sigma_{ij}} E_{ijkl} \frac{\partial f}{\partial \sigma_{kl}} + \frac{2}{3} C \frac{\partial f}{\partial \sigma_{ij}} \frac{\partial f}{\partial \sigma_{ij}} - \gamma \frac{\partial f}{\partial \sigma_{ij}} M_{minj} M_{mrns} X_{rs} - \frac{\partial f}{\partial \phi_{ij}} \frac{\partial f}{\partial Y_{ij}} + \frac{b\left(Q-R\right)}{\left(1-\phi_{eq}\right)^2} \tag{3.110}$$

$$a_{12} = \frac{\partial f}{\partial \sigma_{ij}} E_{ijkl} \frac{\partial g}{\partial \sigma_{kl}} - \frac{\partial f}{\partial \phi_{ij}} \frac{\partial g}{\partial Y_{ij}} \tag{3.111}$$

and

$$b_1 = \frac{\partial f}{\partial \sigma_{ij}} E_{ijkl} \dot{\varepsilon}_{kl} \tag{3.112}$$

where

$$\frac{\partial f}{\partial \sigma_{ij}} = \frac{\partial f}{\partial \bar{\sigma}_{mn}} \frac{\partial \bar{\sigma}_{mn}}{\partial \sigma_{ij}} = M_{minj} \frac{\partial f}{\partial \bar{\sigma}_{mn}} \quad \text{with} \quad \frac{\partial f}{\partial \bar{\sigma}_{mn}} \equiv \frac{3}{2} \frac{\bar{\tau}_{mn} - \bar{X}_{mn}}{\sqrt{\frac{3}{2}\left(\bar{\tau}_{kl} - \bar{X}_{kl}\right)\left(\bar{\tau}_{kl} - \bar{X}_{kl}\right)}} \tag{3.113}$$

$$\begin{aligned} \frac{\partial f}{\partial \phi_{ij}} &\equiv \frac{\partial f}{\partial \sigma_{mn}} \frac{\partial \sigma_{mn}}{\partial \phi_{ij}} + \frac{\partial f}{\partial X_{mn}} \frac{\partial X_{mn}}{\partial \phi_{ij}} + \frac{\partial f}{\partial R} \frac{\partial R}{\partial \phi_{ij}} \\ &= M_{mrns} \frac{\partial f}{\partial \bar{\sigma}_{rs}} J_{mpnqij} M_{pkql} \left(\sigma_{kl} - X_{kl}\right) + \frac{\phi_{ij}}{\left(1-\phi_{eq}\right)^2} R \end{aligned} \tag{3.114}$$

$$\frac{\partial f}{\partial Y_{ij}} \equiv \frac{\partial f}{\partial \sigma_{mn}} \frac{\partial \sigma_{mn}}{\partial Y_{ij}} = \frac{\partial f}{\partial \sigma_{mn}} \left(\frac{\partial Y_{ij}}{\partial \sigma_{mn}} \right)^{-1} \quad \text{with} \quad \frac{\partial Y_{ij}}{\partial \sigma_{mn}} = M_{kplq} J_{kplqij} \varepsilon^{E}_{mn} \tag{3.115}$$

On the other hand, the consistency condition for the damage, $\dot{g} = 0$, can be written as follows:

$$\dot{g} \equiv \frac{\partial g}{\partial Y_{ij}} \dot{Y}_{ij} + \frac{\partial g}{\partial H_{ij}} \dot{H}_{ij} + \frac{\partial g}{\partial K} \dot{K} = 0 \tag{3.116}$$

However, since the damage driving force $\boldsymbol{Y}$ is a function of $\boldsymbol{\sigma}$ and $\boldsymbol{\phi}$ (see Eq. (3.71)), the damage consistency condition can be rewritten as follows:

$$\dot{g} \equiv \frac{\partial g}{\partial \sigma_{ij}} \dot{\sigma}_{ij} + \frac{\partial g}{\partial H_{ij}} \dot{H}_{ij} + \frac{\partial g}{\partial K} \dot{K} + \frac{\partial g}{\partial \phi_{ij}} \dot{\phi}_{ij} = 0 \tag{3.117}$$

Making use of Eqs. (3.78), (3.80), (3.101), (3.103), (3.104), and (3.105) along with the chain rule, it can be shown, after some manipulation, that the consistency condition, Eq. (3.117), gives the following relation between $\dot{\lambda}^{p}$ and $\dot{\lambda}^{d}$, such that:

$$a_{21}\dot{\lambda}^{p} + a_{22}\dot{\lambda}^{d} = b_2 \tag{3.118}$$

where

$$a_{21} = \frac{\partial g}{\partial \sigma_{ij}} E_{ijkl} \frac{\partial f}{\partial \sigma_{kl}} - \frac{\partial g}{\partial \phi_{ij}} \frac{\partial f}{\partial Y_{ij}} \tag{3.119}$$

$$a_{22} = \frac{\partial g}{\partial \sigma_{ij}} E_{ijkl} \frac{\partial g}{\partial \sigma_{kl}} - d \frac{\partial g}{\partial Y_{ij}} H_{ij} - \frac{\partial g}{\partial \phi_{ij}} \frac{\partial g}{\partial Y_{ij}} + c\left(q - K\right) + a \tag{3.120}$$

and

$$b_2 = \frac{\partial g}{\partial \sigma_{ij}} E_{ijkl} \dot{\varepsilon}_{kl} \tag{3.121}$$

where

$$\frac{\partial g}{\partial \sigma_{ij}} \equiv \frac{\partial g}{\partial Y_{mn}} \frac{\partial Y_{mn}}{\partial \sigma_{ij}} = \varepsilon_{ij}^{E} \frac{\partial g}{\partial Y_{mn}} M_{kplq} J_{kplqmn} \tag{3.122}$$

$$\begin{aligned} \frac{\partial g}{\partial \phi_{ij}} &\equiv \frac{\partial g}{\partial Y_{mn}} \frac{\partial Y_{mn}}{\partial \phi_{ij}} + \frac{\partial g}{\partial H_{mn}} \frac{\partial H_{mn}}{\partial \phi_{ij}} + \frac{\partial g}{\partial K} \frac{\partial K}{\partial \phi_{ij}} \\ &= \frac{\partial g}{\partial Y_{mn}} \left(\bar{\Psi}^{E} M_{kalb} M_{rpsq} J_{arbsij} J_{kplqmn} - \frac{\partial H_{mn}}{\partial \phi_{ij}} \right) - a_2 \frac{\phi_{ij}}{\phi_{eq}} \end{aligned} \tag{3.123}$$

The plastic multiplier, $\dot{\lambda}^{p}$, and the damage multiplier, $\dot{\lambda}^{d}$, can be found from the linear system of equations given by Eqs. (3.109) and (3.118) such that:

$$\begin{Bmatrix} \dot{\lambda}^{p} \\ \dot{\lambda}^{d} \end{Bmatrix} = \frac{1}{\Delta} \begin{bmatrix} a_{22} & -a_{12} \\ -a_{21} & a_{11} \end{bmatrix} \begin{Bmatrix} b_1 \\ b_2 \end{Bmatrix} \tag{3.124}$$

where

$$\Delta = a_{11} a_{22} - a_{12} a_{21} \tag{3.125}$$

3.4.5 The Elasto-Plastic-Damage Tangent Stiffness

Substituting $\dot{\lambda}^{p}$ and $\dot{\lambda}^{d}$ from Eq. (3.124) into Eq. (3.78), the evolution equation for the inelastic strain rate $\dot{\boldsymbol{\varepsilon}}^{I}$ can be written in the following form:

$$\dot{\varepsilon}_{ij}^{I} = \chi_{ijkl} \dot{\varepsilon}_{kl} \tag{3.126}$$

where $\boldsymbol{\chi}$ is a fourth-order tensor and is expressed as follows:

$$\chi_{ijkl} = P_{ijkl} + Z_{ijkl} \tag{3.127}$$

where

$$P_{ijkl} = \frac{\partial f}{\partial \sigma_{ij}} A_{rs} E_{rskl} \tag{3.128}$$

$$Z_{ijkl} = \frac{\partial g}{\partial \sigma_{ij}} B_{rs} E_{rskl} \tag{3.129}$$

$$A_{rs} = \frac{1}{\Delta}\left[a_{22} \frac{\partial f}{\partial \sigma_{rs}} - a_{12} \frac{\partial g}{\partial \sigma_{rs}} \right] \tag{3.130}$$

$$B_{rs} = \frac{1}{\Delta}\left[a_{11} \frac{\partial g}{\partial \sigma_{rs}} - a_{21} \frac{\partial f}{\partial \sigma_{rs}} \right] \tag{3.131}$$

Substitution of Eqs. (3.126) and Eq. (3.33) into Eq. (3.108), yields the following:

$$\dot{\sigma}_{ij} = D_{ijkl} \dot{\varepsilon}_{kl} \tag{3.132}$$

where $\boldsymbol{D}$ represents the elasto-plastic-damage tangent stiffness given by:

$$D_{ijkl} = E_{ijkl} - E_{ijmn} \chi_{mnkl} \tag{3.133}$$

The tangent stiffness $\boldsymbol{D}$ has two possible expressions, such that:

$$D_{ijkl} = \begin{cases} \overline{E}_{ijkl} & \text{if } \; f < 0 \; or \; \dot{f} < 0 \; \& \; g < 0 \; or \; \dot{g} < 0 \\ E_{ijkl} - E_{ijmn} \chi_{mnkl} & \text{if } \; f = 0 \Leftrightarrow \dot{\lambda}^p \dot{f} = 0 \; or \; g = 0 \Leftrightarrow \dot{\lambda}^d \dot{g} = 0 \end{cases} \tag{3.134}$$

The above expression signifies that $\boldsymbol{D} = \overline{\boldsymbol{E}}$ if there is no damage and no plastic flow; and $\boldsymbol{D} = \boldsymbol{E}$ if there is total crack closure, total void contraction, and no plastic flow.

The set of constitutive equations for the proposed model with damage and plasticity coupling are summarized in Table 3.1.

3.5 Qualitative and Quantitative Results

The pure damage and the coupled plastic-damage model behavior are examined in the sequel for the case of isotropic damage. The new features that the proposed model is attempting to represent are illustrated by providing qualitative and quantitative plots of stress versus strain.

Table 3.1 Constitutive equations of the proposed coupled elasto-plastic-damage model.

i. Elastic stress-strain relationship

$$\boldsymbol{\sigma} = \bar{\boldsymbol{E}} : \left(\boldsymbol{\varepsilon} - \boldsymbol{\varepsilon}^{ed} - \boldsymbol{\varepsilon}^{p} - \boldsymbol{\varepsilon}^{id} \right)$$

ii. Damage stress-strain relationship

$$\boldsymbol{\sigma} = \boldsymbol{E} : \left(\boldsymbol{\varepsilon} - \boldsymbol{\varepsilon}^{p} - \boldsymbol{\varepsilon}^{id} \right) \quad \text{with} \quad \boldsymbol{E} = \boldsymbol{M} : \bar{\boldsymbol{E}} : \boldsymbol{M}$$

iii. Flow-Rules

$$\dot{\boldsymbol{\varepsilon}}^{p} = \dot{\lambda}^{p} \frac{\partial f}{\partial \boldsymbol{\sigma}}, \quad \dot{\boldsymbol{\varepsilon}}^{id} = \dot{\lambda}^{d} \frac{\partial g}{\partial \boldsymbol{\sigma}}, \quad \dot{\boldsymbol{\phi}} = \dot{\lambda}^{p} \frac{\partial f}{\partial \boldsymbol{Y}} + \dot{\lambda}^{d} \frac{\partial g}{\partial \boldsymbol{Y}}$$

iv. Isotropic and kinematic hardening laws

a. Plasticity

$$\dot{R} = b\left[Q - R \right] \dot{p}, \qquad \dot{\boldsymbol{X}} = \frac{2}{3} C \dot{\boldsymbol{\varepsilon}}^{p} - \gamma \dot{p}\, \boldsymbol{M} : \boldsymbol{M} : \boldsymbol{X}$$

b. Damage

$$\dot{K} = c\left(q - K \right) \dot{r}, \qquad \dot{\boldsymbol{H}} = \left(a \frac{\partial g}{\partial \boldsymbol{Y}} - d\boldsymbol{H} \right) \dot{r}$$

v. Yield and damage conditions

$$f = \sqrt{\tfrac{3}{2} \left(\bar{\boldsymbol{\tau}} - \bar{\boldsymbol{X}} \right) : \left(\bar{\boldsymbol{\tau}} - \bar{\boldsymbol{X}} \right)} - \sigma_{yp} - \bar{R} \le 0;$$

$$g = \sqrt{\left(\boldsymbol{Y} - \boldsymbol{H} \right) : \left(\boldsymbol{Y} - \boldsymbol{H} \right)} - l_{d} - K \le 0$$

with $\boldsymbol{Y} = 2\bar{\Psi}^{E} \boldsymbol{M} : \boldsymbol{J}$

vi. Kuhn-Tucker conditions

$$\dot{\lambda}^{p} \ge 0, \quad f \le 0 \quad \Leftrightarrow \dot{\lambda}^{p} f = 0$$

$$\dot{\lambda}^{d} \ge 0, \quad g \le 0 \quad \Leftrightarrow \dot{\lambda}^{d} g = 0$$

vii. Consistency conditions

$$\dot{f} = 0 \text{ if } f = 0 \quad \& \quad \dot{g} = 0 \text{ if } g = 0$$

viii. Tangent stiffness

$$\boldsymbol{D} = \begin{cases} \bar{\boldsymbol{E}} & \text{if } f < 0 \text{ or } \dot{f} < 0 \ \& \ g < 0 \text{ or } \dot{g} < 0 \\ \boldsymbol{E} - \boldsymbol{E} : \boldsymbol{\chi} & \text{if } f = 0 \Leftrightarrow \dot{\lambda}^{p} \dot{f} = 0 \ \& \ g = 0 \Leftrightarrow \dot{\lambda}^{d} \dot{g} = 0 \end{cases}$$

3.5.1 The Case of Pure Isotropic Damage

In this section some properties of the damage model proposed in Section 3.4.3.2 are investigated for some simple uniaxial processes using a dissipation mechanism produced by the damage potential only. The damage criterion with linear isotropic damage hardening is considered such that Eq. (3.101) can be expressed as follows:

$$g = \frac{\bar{E}(1-\phi)^3}{(1+\phi)^2}\varepsilon^2 - l_d - q\phi = 0 \tag{3.135}$$

where $\varepsilon = \varepsilon^e + \varepsilon^{ed} + \varepsilon^{id}$ is the total strain, l_d is the damage threshold, and q is the damage hardening modulus. The evolution of the damage variable ϕ in uniaxial extension can be obtained from Eq. (3.135) for a given ε, l_d, and q. The limit uniaxial strain and stress at which damage initiates are obtained by setting $\phi = 0$ in Eq. (3.135) such that:

$$\varepsilon_o = \sqrt{l_d / \bar{E}}\,, \qquad \sigma_o = \sqrt{\bar{E}\, l_d} \tag{3.136}$$

The elastic strain, ε^e, the elastic-damage strain, ε^{ed}, and the inelastic-damage strain, ε^{id}, can be obtained from the relations presented in Section 3.3.1 and Eq. $(3.79)_2$ such that:

$$\varepsilon^e = \frac{(1-\phi)^3}{(1+\phi)}\varepsilon\,, \qquad \varepsilon^{ed} = \frac{(1-\phi)-(1-\phi)^3}{(1+\phi)}\varepsilon\,, \qquad \varepsilon^{id} = \frac{2\phi}{1+\phi}\varepsilon \tag{3.137}$$

For $\phi = 0$, $\varepsilon^e = \varepsilon$ and $\varepsilon^{ed} = \varepsilon^{id} = 0$, the stress relation follows from the elastic constitutive relation:

$$\sigma = D_{\text{sec}}\varepsilon \quad \text{with } D_{\text{sec}} = \frac{(1-\phi)^3}{(1+\phi)}\bar{E} \tag{3.138}$$

The stress-strain curves are shown in Figure 3.7 for different values of the damage threshold l_d and the damage hardening modulus q. It is evident that the model allows simulating a continuous change from hardening to softening as well as the reduction in the stiffness. It is noteworthy that the energy necessary to initiate the damaged state (that can be interpreted as fracture energy G_f) is finite, in fact it is expressed as follows:

$$G_f = \int_o^{\varepsilon_o} \sigma \, \mathrm{d}\varepsilon = \frac{1}{2}\bar{E}\varepsilon_o^2 = \frac{1}{2}l_d \tag{3.139}$$

Therefore, for $q = 0$, Eq. (3.135) characterizes a fracture-type criterion. Moreover, it can be noted from Figure 3.7(b) that for $q = 0$ (i.e. no damage hardening), for each ϕ there is a

unique value of stress; while for $q \neq 0$ (i.e. with damage hardening), for each ϕ there are two possible stress values. Therefore, due to the presence of damage the application of this model to structural problems will cause strain localization with the consequent mesh-dependency of the numerical results. Several regularization approaches, either in time or space, have been proposed in the literature to accommodate this problem (see Voyiadjis et al., 2001). However,

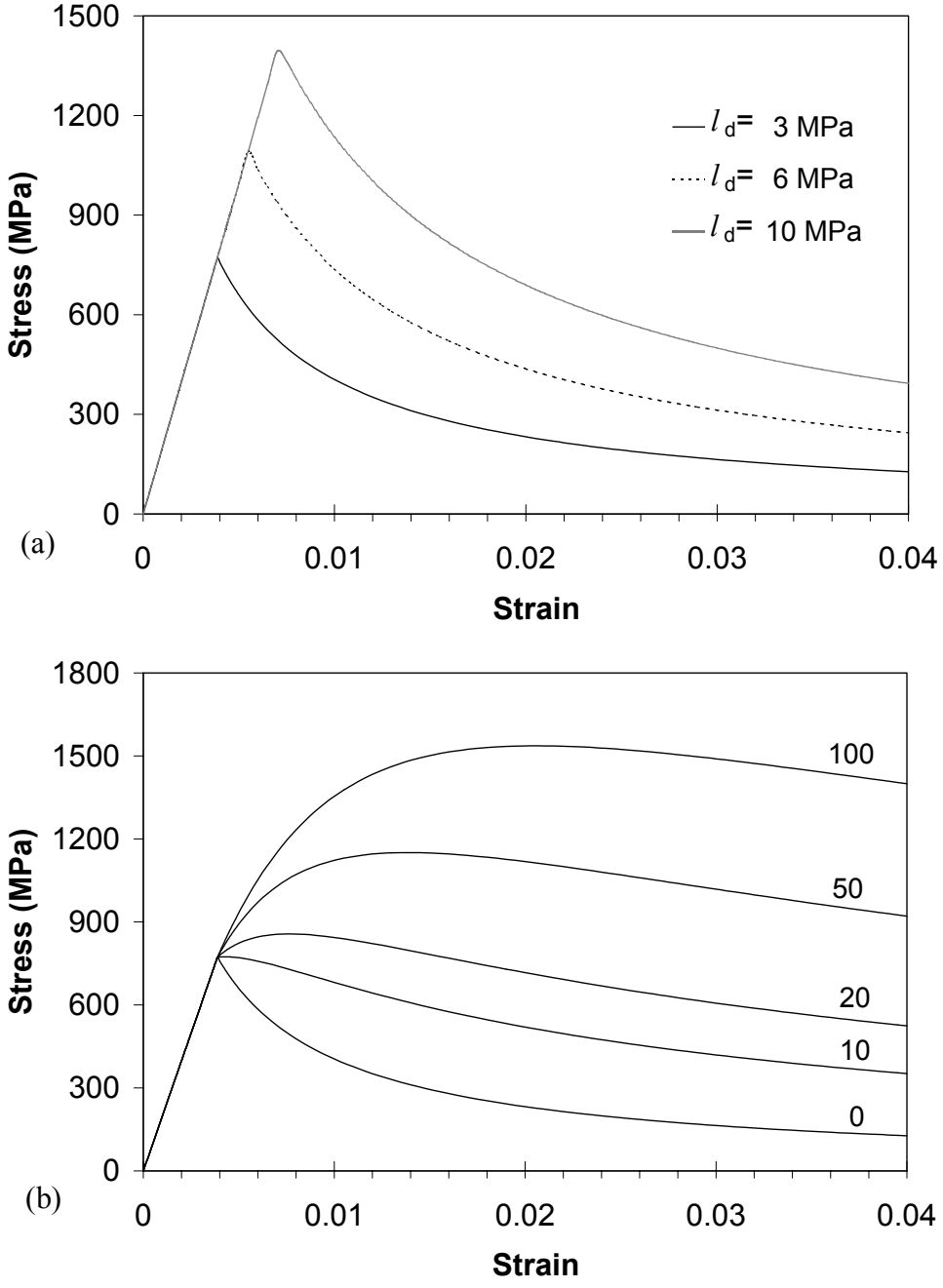

Figure 3.7 Influence of the (a) l_d parameter and (b) q (Mpa) parameter for $\bar{E}$=199 GPa.

the purpose of this study is to introduce the model and the possible strategies for coping with strain localization are beyond the goal of the present work.

The loading-unloading behavior is considered in Figure 3.8(a). When damage occurs, it can be seen upon unloading that there is a permanent strain in the stress free state. This qualitatively agrees with the experimental observations in concrete (Van Mier, 1984), where

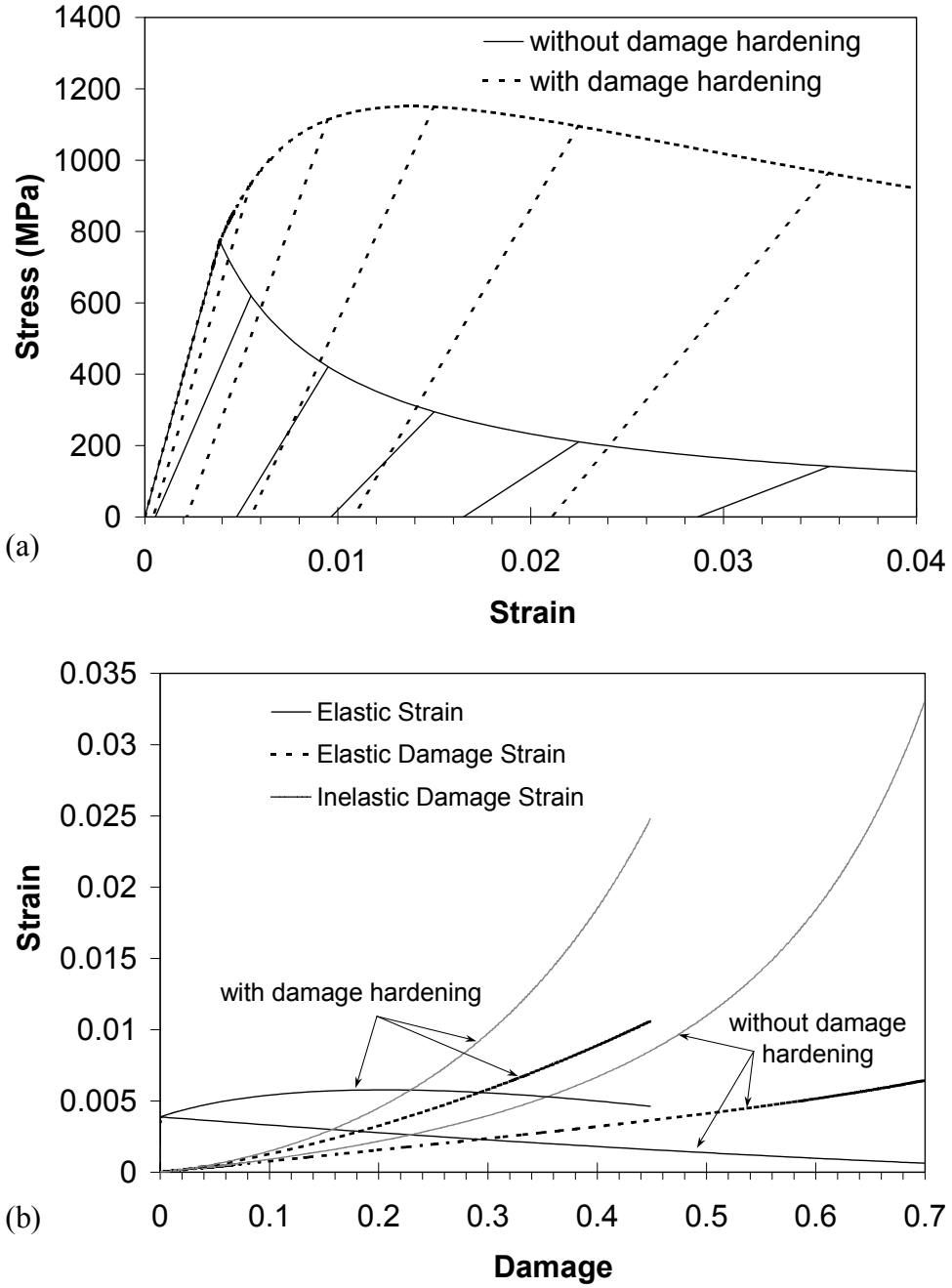

Figure 3.8 Damage Hardening effect. (a) Loading-unloading uniaxial tensile process, (b) variation of different type of strains with damage, for $\overline{E}$ =199 GPa and l_d =3 MPa.

plasticity is assumed to be negligible. The stress-strain plot in Figure 3.8(a) with damage hardening is obtained for very large value of $q = 50\,MPa$ so that the secant stiffness, $D_{\sec}$, after initiation of damage does not degrade immediately, as it has been observed in some experimental tests on concrete. Hardening then decreases fast as soon as damage localization develops. Figure 3.8(b) shows the variation of the different coupled-damage strains with respect to the damage variable ϕ. Figure 3.8 shows an important feature of the proposed damage model that has not been considered by most of the previous models. Furthermore, it can be seen that for the same corresponding imposed strain, the elastic-damage modulus is bigger for pure damage with hardening than without hardening. This implies an increase in the material strength due to the interaction between microdamages. This is also a new aspect that was not provided by many in previous damage models.

The influence of the hardening modulus q is shown in Figure 3.9 for $l_d = 3.0\,MPa$ and $\bar{E} = 199\,GPa$. The evolution of ϕ and the elastic-damaged modulus E are also reported. Increasing values of q determine stronger reduction in ϕ and stronger increase in E. The parameter q particularly influences the degradation of the elastic modulus and the concavity of the stress-strain curve $E(\phi)$ that can be obtained from experiments (Figure 3.9).

3.5.2 Coupled Plasticity and Damage: Application to High Strength Steel

In this section the experimental results of Hesebeck (2001) for a high strength steel are numerically simulated using the proposed model. The tested high strength steel 30CrNiMo8 contains 33% carbon. Further details of the chemical composition are documented in Hesebeck (2001). In the mechanical testing, force controlled tension tests with partial unloadings were performed at a stress rate of $\dot{\sigma} = 30 MPa/s^{-1}$. The resulting stress versus strain curve obtained by Hesebeck (2001) is plotted in Figure 3.10.

Considering the fact that there are no unified experimental methods developed to quantify the damage variable, one can obtain ϕ with sufficient precision by evaluating the unloading (i.e. the decrease in the stiffness) in the stress-strain curve, such that one can write from Eq. (3.22) the following expression:

$$\phi = 1 - \sqrt{\frac{E}{\bar{E}}} \tag{3.140}$$

Voyiadjis and Venson (1995) proposed the use of the sectioned specimens together with the use of the SEM for the determination of crack densities. However, different interpretations of the experimental damage variable have been made by Hesebeck (2001), which is based on the strain equivalence principle (i.e. $E = \bar{E}(1-\phi)$). However, the strain energy equivalence is considered in the present work. The result for the damage variable using Eq. (3.140) is plotted in Figure 3.11 versus the elastic-damage modulus, E.

Identification of the material constants associated with any proposed material model is one of the most challenging issues for researchers in order to obtain better representation of their material models. The identification approach of the material constants for the evolution

equations outlined in the previous sections is based on the experimental results in Figures 3.10, 3.11, and 3.12 by using the least-square minimization method.

Young's modulus, Poisson's ratio, and the initial flow stress were pre-determined by Hesebeck (2001) as $\overline{E} = 199\,GPa$, $\nu = 0.3$, and $\sigma_{yp} = 870\,MPa$, respectively. The object of the identification process here is to identify the four parameters (Q, b, C, γ) of Eqs. (3.92) and (3.99), characterizing the plastic isotropic and kinematic hardening, and the five

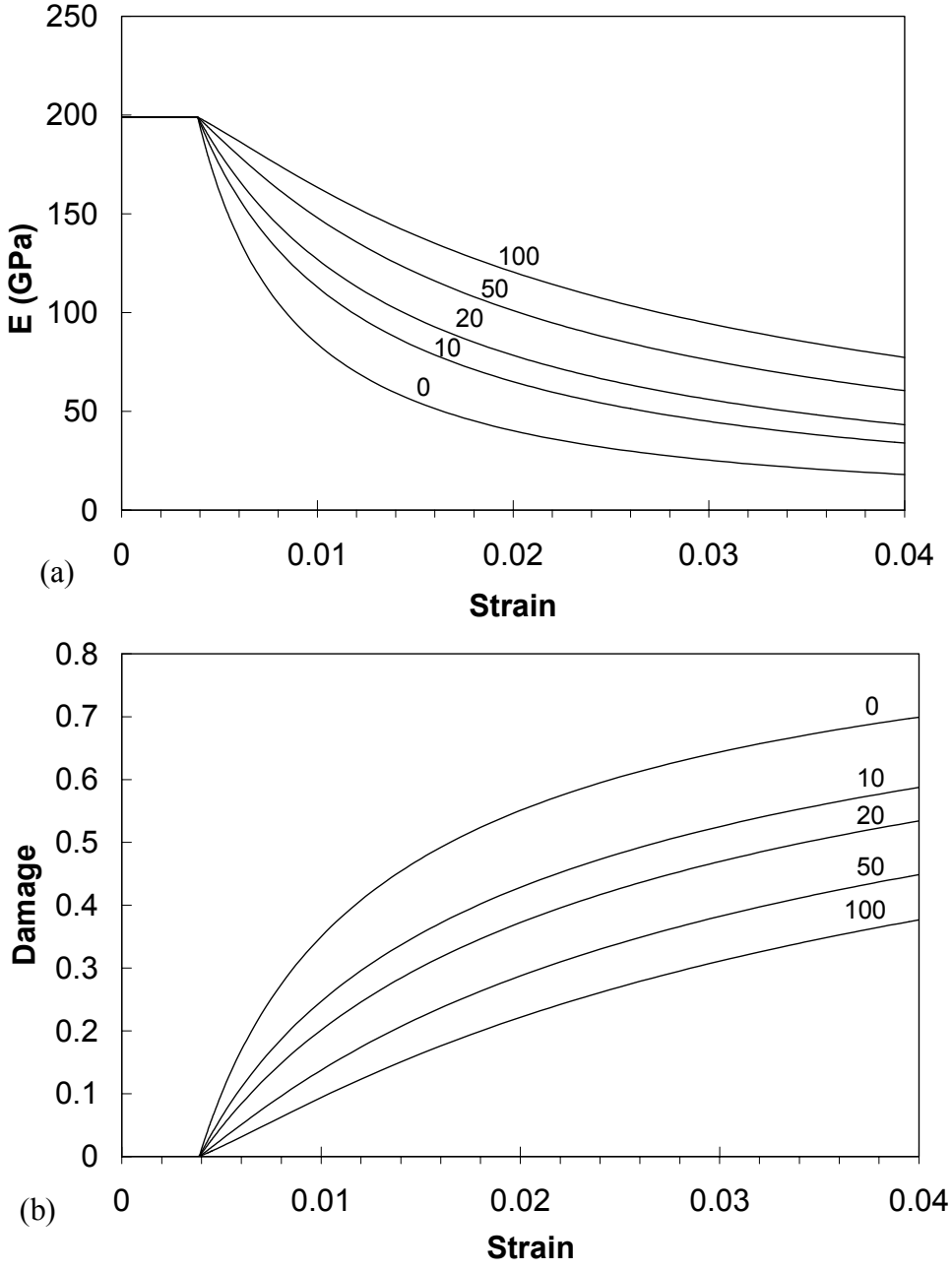

Figure 3.9 (a), (b) Influence of q (MPa) parameter for $\overline{E}$ =199 GPa and l_d =3 MPa.

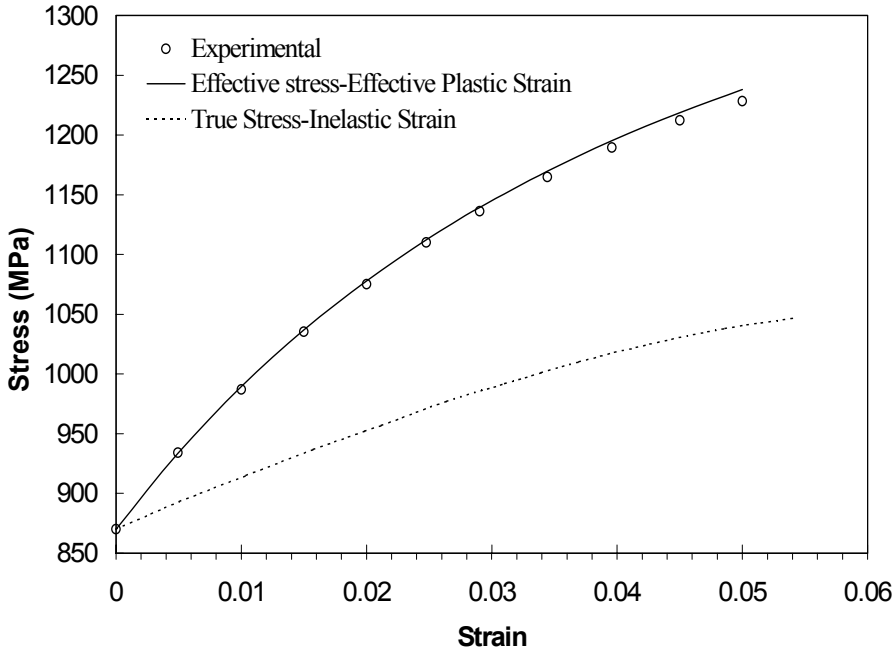

Figure 3.10 Stress-strain diagram for damaged and effective undamaged 30CrNiMo8-steel as compared to the experimental data.

parameters (l_d, q, c, d, a) of Eqs. (3.101), (3.104), and (3.105), characterizing the initial damage threshold, and damage isotropic and kinematic hardening. The plasticity hardening parameters are determined using the effective stress-effective and plastic strain curve in Figure 3.10, while the damage parameters are determined using all the experimental data in Figures 3.10, 3.11, and 3.12. The obtained material parameters are listed in Table 3.2.

Preliminary results not reported here revealed that the effective stress-effective plastic strain curve could be obtained with reasonable agreement with the experimental data by considering only the isotropic hardening evolution. However, this is only by using different material parameters than those listed in Table 3.2. Nevertheless this is not a problem for the practical applicability of the developed model. The emphasis of this work is to understand better the different deformation morphologies that affect the material behavior by considering their synergetic effects. Therefore, the influence of the different cooperative phenomena on plasticity and damage growth are discussed here. The curves plotted in Figures 3.13-3.15 represent the synergetic effects of the combined isotropic and kinematic hardening associated

Table 3.2 The plasticity and damage material parameters for 30CrNiMo8 high strength steel.

Mechanism	Isotropic Hardening	Kinematic Hardening	Initial Flow Threshold
Plasticity	$Q = 409\,MPa$ $b = 9.3$	$C = 15,000\,MPa$ $\gamma = 37$	$\sigma_{yp} = 870\,MPa$
Damage	$q = 8.2\,MPa$ $c = 5.2$	$a = 14.70\,MPa$ $d = 0.11$	$l_d = 3.8\,MPa$

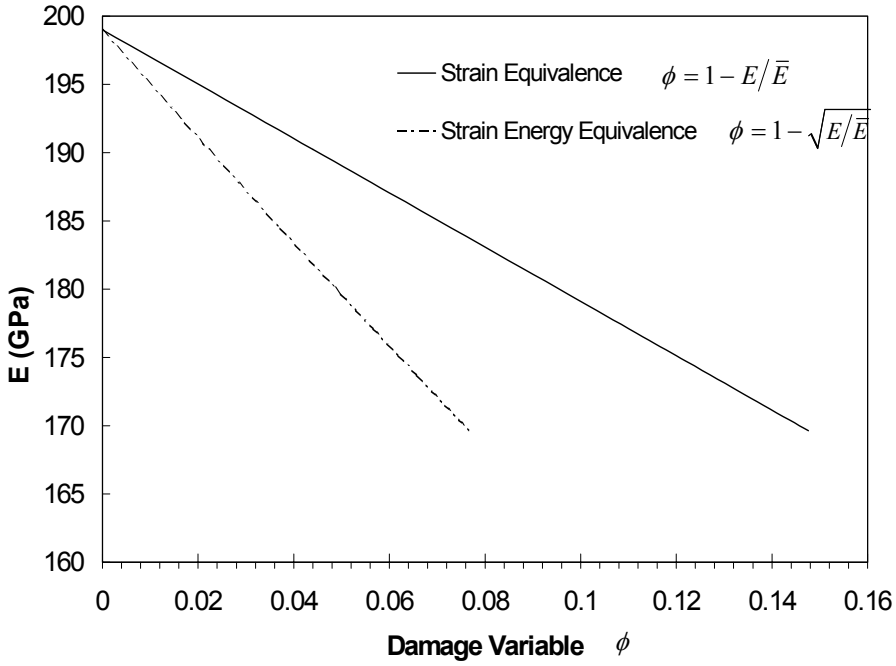

Figure 3.11 Elastic-damage modulus (E) versus damage variable (ϕ).

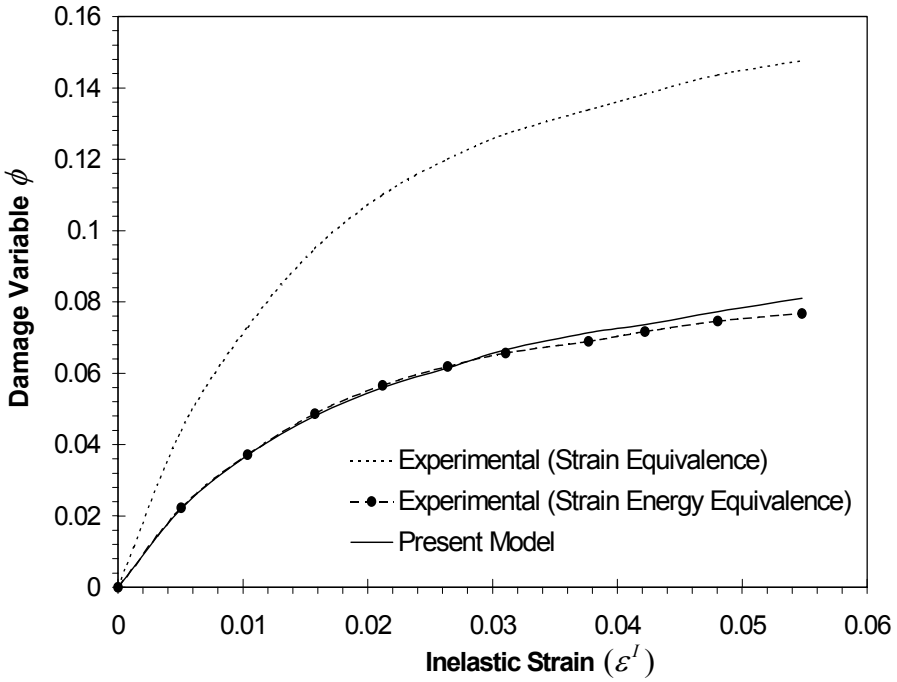

Figure 3.12 Comparison of experiments by Hesebeck (2001) with the simulated data of the present work for the damage variable versus the inelastic strain.

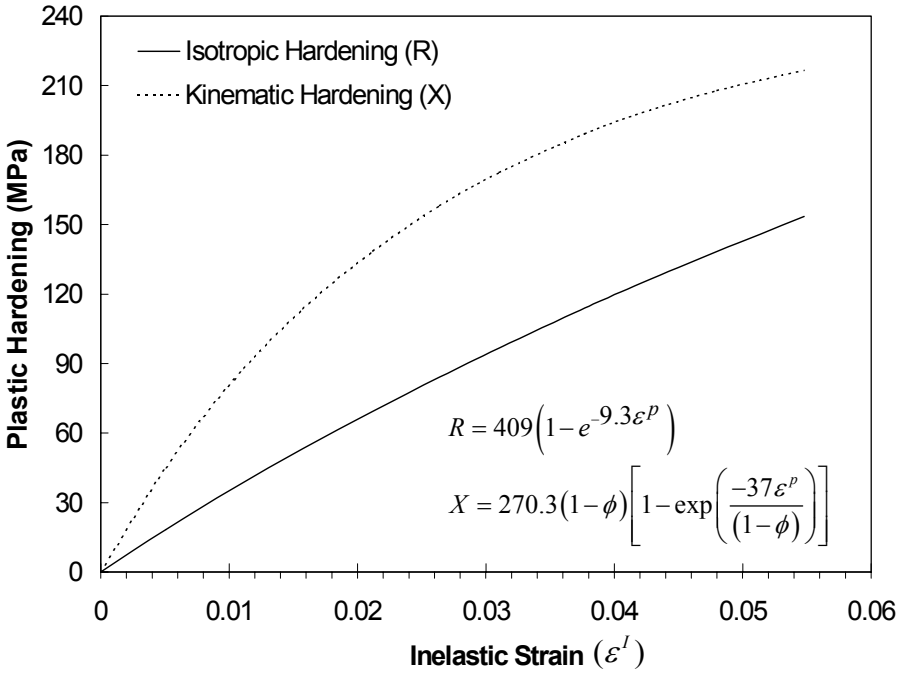

Figure 3.13 Evolution of the plasticity dissipative forces using the present model.

with plasticity, combined isotropic and kinematic hardening associated with damage, and damage mechanisms.

Figure 3.10 depicts the resulting effective stress versus the effective plastic strain curve of the proposed model, thus revealing a very good agreement with the experimental data. Also, the true stress ($\sigma = (1-\phi)\bar{\sigma}$) versus the inelastic strain ($\varepsilon^I = \bar{\varepsilon}^p/(1-\phi)$) curve is shown in Figure 3.10. The results of the present work for the damage variable (ϕ) versus the inelastic strain (ε^I) are shown in Figure 3.12 while considering the experimental calculation of the damage variable and using both the strain equivalence and the strain energy equivalence principles. Also for this type of data it becomes apparent that the proposed model is able to give a good agreement with the experimental data for the material under consideration. High nonlinear dependency between ϕ and ε^I is noticed in Figure 3.10, which agrees well with the experimental observations.

The evolution of the plasticity dissipative forces R and X, and the damage dissipative forces K, H, and Y are shown in Figures 3.13 and 3.14, respectively. Closed form expressions have been derived for the plasticity and damage hardening forces by integrating Eqs. (3.92), (3.99), (3.104), and (3.105) over the uniaxial tensile stress-strain data. The damage force Y is simplified for the one-dimensional case by using Eq. (3.71).

The calculated additive decomposition of the total elastic strain (ε^E) into the ordinary elastic strain (ε^e) and the elastic-damage strain (ε^{ed}) as a function of ϕ is shown in Figure 3.15(a). In addition, the calculated additive decomposition of the total inelastic strain (ε^I) into the plastic strain (ε^p) and the inelastic-damage strain (ε^{id}) as a function of ϕ is shown in Figure 3.15(b). Figure 3.15 shows qualitatively the correct mechanical behavior as anticipated in the discussion outlined in Section 3.2.

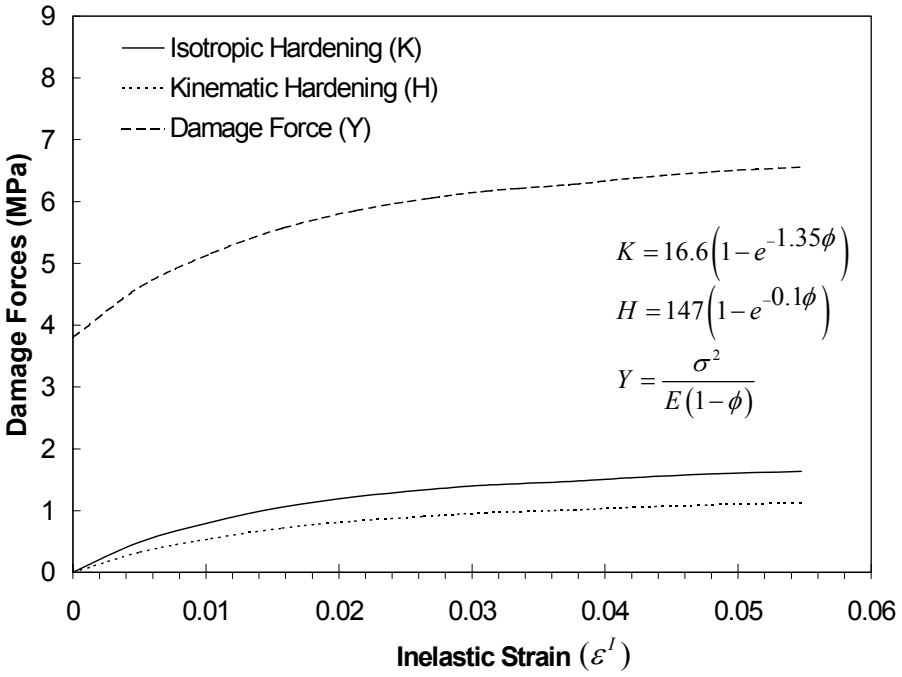

Figure 3.14 Evolution of the damage dissipative forces using the present model.

Although this study is restricted to small strains, usually up to 2-4%, the results in Figures 3.10-3.15 are extended to inelastic strains up to 6%. However, the proposed model is in reasonable quantitative agreement with the experimental data for uniaxial loading and exhibits a qualitatively correct behavior for the evolution of the different strain types. Moreover, one will find in the literature considerable fewer published experimental results for multiaxial loadings. In this work uniaxial tension experimental data with unloadings are used to obtain the constitutive parameters of the proposed model. The reduction in the elastic stiffness, particularly, has been measured from the uniaxial case.

In the current chapter the systematic construction of a thermodynamic consistent model for ductile materials, which provides a strong coupling between plasticity and damage, is presented. The model considers the different interaction mechanisms exhibited by the plasticity and the damage morphologies. Plasticity and damage combined isotropic and kinematic hardening are considered. In addition, an additive decomposition of the total strain into elastic, plastic, and damage parts is proposed in this chapter. Although microstructural arguments are used to motivate many aspects of the formulation, the fact remains that the formulation is phenomenological. The material behavior is described through a suitable set of internal variables and whose relation to micromechanical structure and processes is not exactly defined.

A strong coupling between the two dissipative processes, plasticity and damage, is implemented. This strong coupling is assessed by using two separate plasticity and damage surfaces with separate non-associated flow rules in such a way that both damage and inelastic flow rules are dependent on the plastic and damage potentials. Two damage mechanisms are considered, one mechanism is coupled with plasticity, and while the other one occurs independent of plastic deformation. The dissipation function of the latter occurs in both the elastic and plastic domains. Even though the verification is based on a limited set of data,

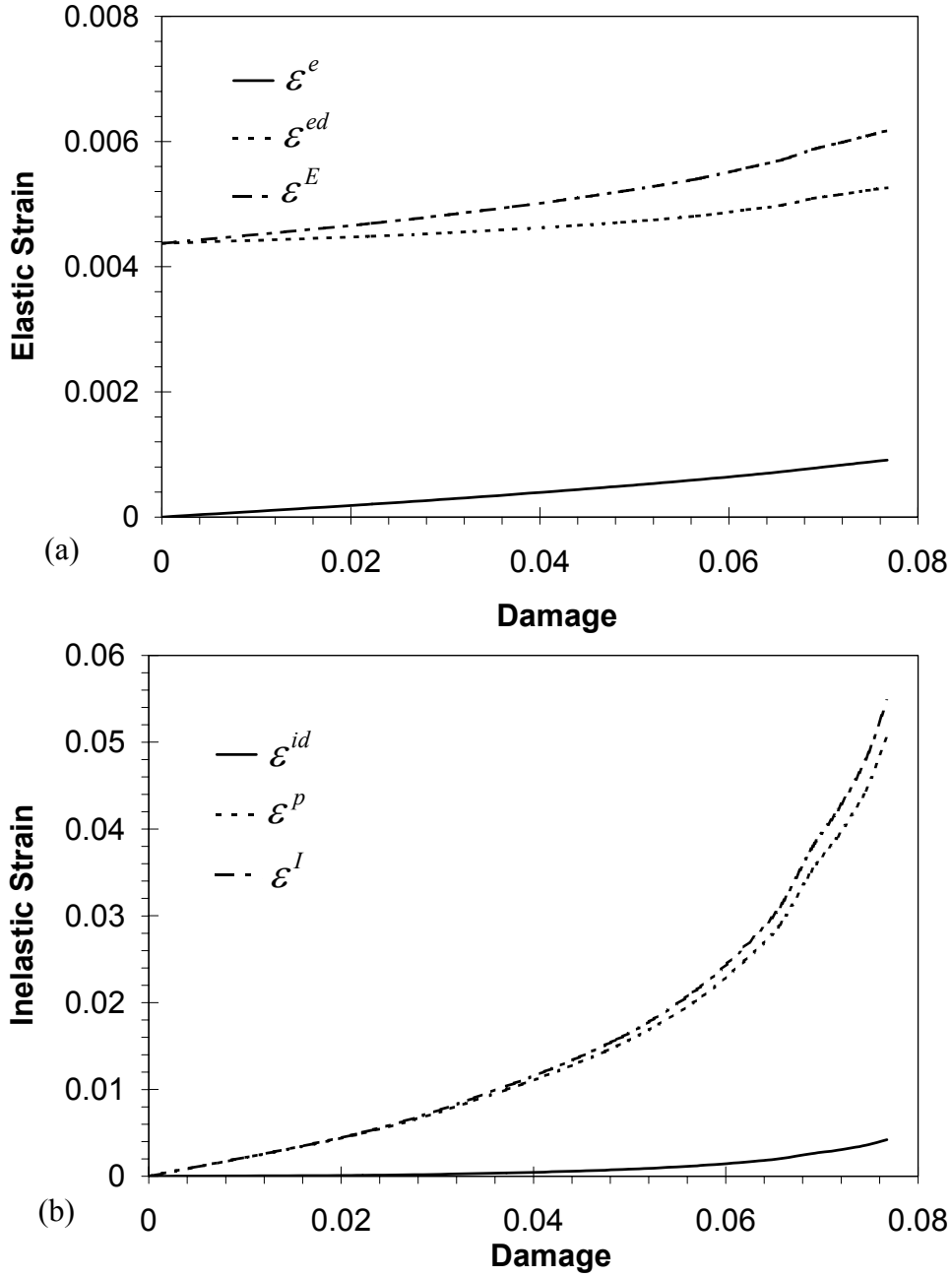

Figure 3.15 Variation of the strain decomposition with the damage variable. (a) Elastic strain decomposition, (b) inelastic strain decomposition.

namely that of uniaxial stress and strain, this could specifically motivate experimentalists to look for the new features that would provide justification for the approach used in the current study.

Explicit treatment of the microdamage distribution (spacing and orientation) and size, which have a considerable influence on the interaction between defects, will be addressed in the coming chapters. Chapter 5 is directed for implementing the proposed model in a finite deformation framework to model problems that exhibit non-homogenous deformation. These

additional investigations should be based on the results of the micromechanical characterization of the materials that exhibit heterogenous behavior. Moreover, the problem of size effect, strain localization, and mesh dependency, typical of plasticity and damage evolution, is not adressed in this chapter. Some of these aspects are presented in the coming chapters using the framework of this chapter and the gradient-depndent theories. The ordinary plasticity and damage consistutive relations with which Chapter 2 and this chapter have been concerned cannot capture such problems of size effects, but the gradient-dpendent theory is a continuum theory that can.